NOVEL MEMBRANE BIOFILM REACTOR FOR GROUNDWATER TREATMENT AND REMEDIATION

FINAL REPORT

Prepared by

Samer Adham, Kuang-ping Chiu, and Geno Lehman
MWH
300 North Lake Avenue, Suite 1200, Pasadena, CA 91101

and

Bruce Rittmann, and Jinwook Chung
Northwestern University
2145 Sheridan Road, Evanston, IL 60208

Sponsored by:
National Water Research Institute

CONTENTS

TABLES

FIGURES

ABBREVIATIONS

ADP	adenosine diphosphate
ATP	adenosine triphosphate
°C	degrees Celsius
CA	chloroethane
CaDHS	California Department of Health Services
CaDHS	California Department of Health Services
CF	chloroform
CFD	computational fluid dynamics
CM	chloromethane
Cr	chromium
DCA	dichloroethane
DCE	dichloroethene
DCM	dichloromethane
EPA	Environmental Protection Agency
FID	flame ionization detector
GC	gas chromatograph
H_2	hydrogen
ICP	inductive coupled plasma
M	molar
MBfR	membrane biofilm reactor
MS	mass spectroscopy
NO_3^-	nitrate
NO_2^-	nitrite
PCE	tetrachloroethene
Se	selenium
SPME	solid-phase micro-extraction
SWTR	surface water treatment rule
TCA	trichloroethane
TCA	tricloroethane
TCE	trichlorethene
TCE	trichloroethene
VC	vinyl chloride
VOC	volatile organic compounds
WTC	water treatment committee

EXECUTIVE SUMMARY

BACKGROUND

Increased demands on limited water supplies around the country and abroad have forced many municipalities to consider using ground waters contaminated by a variety of inorganic and organic oxidized contaminants. Additionally, improved analytical techniques have revealed numerous emerging contaminants that were previously not even considered an issue. Biological reduction may provide the most suitable treatment alternative, as many oxidized contaminants are reduced to innocuous or readily removed forms. An innovative process that should be able to treat the wide range of inorganic and organic oxidized contaminants is the hydrogen-based membrane biofilm reactor (MBfR).

The MBfR makes it practical, for the first time, to use H_2 as an electron donor for microbially catalyzed reductions of oxidized contaminants. In the MBfR, H_2 gas is supplied to the inside of special bubbleless membranes. The H_2 gas diffuses through the membrane and is consumed almost immediately after it emerges on the outside by a biofilm that naturally coats the outside wall of the membrane. The bacteria in the biofilm gain energy by oxidizing H_2 coming from inside the membrane and one or more oxidized contaminants coming from the water. Thus, the membrane wall is the meeting place of the bacteria's electron donor and electron acceptor, and it is where the bacteria naturally accumulate as a biofilm. Supplying H_2 by diffusion eliminates the possibility of forming H_2 bubbles and a combustible atmosphere, which have prevented using hydrogen gas in other process configurations. Additionally, H_2 is the least expensive electron donor, is non-toxic to humans, leaves no residual in the water, and is consistent with society's long-term sustainability goal of moving to a hydrogen-based fuel economy.

RESEARCH OBJECTIVES AND STUDY APPROACH

The primary objectives of this project are to evaluate and optimize an innovative process (the MBfR) to treat inorganic and organic oxidized contaminants. The following project goals outline the major tasks of the project:

- Bench-Scale Experiments on Biological Reduction Fundamentals. Conduct fundamental bench-scale experiments to systematically evaluate the potential of the MBfR to remove a variety of oxidized inorganic and organic compounds and understand the micro-ecology behind these systems.
- Influence of Hydraulics. Develop a hydrodynamic model of the existing MBfRs to aid in identifying how the hydraulics of the reactor (flow rates, membrane fiber orientation, influent/effluent configurations, etc) can be used to optimize the system (biofilm thickness, microbial ecology, mass transport, etc).
- Regulatory Approval. Document and identify the specific requirements that need to be satisfactorily addressed for obtaining CaDHS approval of MBfR process for the production of potable water.

STUDY FINDINGS AND CONCLUSIONS

Bench-Scale Experiments with a Range of Oxidized Contaminants

Bench-scale experiments with the H_2-based MBfR documented the potential of the H_2-oxidizing bacteria in an MBfR to reduce a wide range of oxidized inorganic and organic contaminants. Previous research has demonstrated MBfR reduction of nitrate and perchlorate, and the results reported here extend the range to selenate, chromate, chloroform, TCE, and TCA. Reductions occurred quickly in all cases and responded positively to increased H_2 pressure. The systems showed a high degree of versatility towards different oxidized contaminants.

The reduction of Cr(VI) to Cr(III) began within the first two days of Cr(VI) addition. When the hydrogen pressure was increased from 2.5 psi to 4.0 psi, the average reduction of Cr(VI) was increased from 45 to 57%, confirming that chromate reduction is controlled by H_2 availability. When the influent Cr(VI) loading decreased, the average reduction of Cr (VI) increased to 63%, showing the expected trend that Cr(VI) reduction can be made more complete with a lower Cr(VI) loading. Chromate may have inhibited the reduction of sulfate, since almost no sulfide was produced.

Se(VI) was reduced to Se(IV) within one day of Se (VI) addition. Initially, Se (VI) was reduced exclusively to Se (IV), which is completely soluble; then, Se(IV) was reduced to Se^0, which is a solid and retained with the biomass in the MBfR. Similar to the Cr-MBfR, increasing the H_2 pressure from 2.5 to 4 psi increased the Se(VI) reduction from 59 to 83%, while decreasing the selenate loading gave 99% Se(VI) removal. Selenate did not inhibit sulfate reduction, at least not at the concentrations present in the experiments, but a high level of sulfate reduction slowed selenate reduction by competing for H_2.

A series of short-term tests documented that nitrate reduction was not affected by the influent chromate or selenate load; the percentage chromate or selenate removal decreased with increased influent load; increasing H_2 pressure increased the reductions of chromate and selenate; and the optimal pH for chromate and selenate reduction was around 7.0 and 7.5, respectively. Furthermore, the Cr-reducing MBfR was immediately able to reduce selenate, while the Se-reducing MBfR was immediately able to reduce chromate.

When CF was added to a denitrifying MBfR, dechlorination of CF started immediately. DCM was formed transiently as a result of CF reduction, but was transformed to CM and methane after the CF had completely disappeared (3 weeks). When TCE was applied to a denitrifying MBfR, the TCE concentration in the effluent decreased rapidly. cis-1,2-DCE was the major intermediate formed, but it was reduced fully to VC and then to ethene within 3 weeks. The TCA biotransformation rate was somewhat slower than for the other two chlorinated solvents, but it too was reductively dechlorinated within 3.5 weeks. DCA accumulated transiently, and CA gradually increased to become the major end product. The reduction of CA to ethane was not detected, but CA accumulated less than TCA removal.

All three VOCs (CF, TCE, and 1,1,1-TCA) were dechlorinated simultaneously in an MBfR within approximately one month, despite possible inhibitory interactions among the VOCs. At

very high sulfate influent concentrations, partial-dechlorination intermediates accumulated because the competition for H_2 interfered with the full reductive dechlorination of CF, TCE, and TCA.

In summary, the MBfR reduced all oxidized contaminants individually and in combinations. Reduction began immediately and responded as expected to H2 pressure and contaminant loading. Thus, the potential of the MBfR for oxidizing the many oxidized contaminants was fully documented.

Computational Fluid Dynamics Modeling

CFD modeling was used to identify important hydrodynamic characteristics of the bench-scale MBfRs used in this study and pilot-scale MBfRs used in a previous study. CFD modeling of the bench-scale MBfRs was able to reproduce experimentally determined mean residence-time and its variance. The presence of biofilm had little impact on the residence time in tracer experiments or according to CFD modeling. Trajectory analysis showed that the bench-scale MBfR has no dead zones within the main reactor, but the flow velocity is lowest along the outer wall. The shear stress on the membrane, which helps control the biofilm's density and thickness, varies in proportion to the velocity.

For the pilot-scale MBfR, both pilot-scale tracer and CFD modeling show the trend that the higher flow rate generated tighter residence time distribution. The CFD modeling did not accurately simulate the short-circuiting as the results of the tracer tests. More pilot tests are necessary to validate the model.

Final outcomes and interpretations from CFD modeling:
• The MBfR needs a uniform flow distribution that minimized dead zones and wall effects.
• The higher flow velocity increases shear stress, which helps to create a dense, thin biofilm.
• It is desired to have uniform flow distribution system to avoid dead zones or a flow condition with high variance.

Regulatory Approval

A workshop with CaDHS and held at the outset of the project yielded these key issues that need to be addressed by this and other research on the MBfR:

- The need to investigate post-filtration requirements for removing sloughed biomass;
- Demonstrating the need for disinfection; and
- Determining alternative applications beside perchlorate. The WTC suggested that nitrate treatment might be a more immediate application as opposed to perchlorate.

CHAPTER 1

INTRODUCTION

BACKGROUND

Increased demands on limited water supplies around the country and abroad have forced many municipalities to consider the use of groundwaters contaminated by a variety of inorganic and organic oxidized contaminants. Additionally, improved analytical techniques have revealed numerous emerging contaminants that were previously not even considered an issue. The wide range of chemical properties that characterize these compounds have forced many utilities to install multiple physical or chemical unit operations to address each class of compounds. Most of these physical/chemical processes remove the contaminants from the water, only to concentrate them in various residual streams that require special handling or additional processing. Biological reduction may provide a suitable treatment alternative, as many oxidized contaminants are reduced to innocuous, less toxic, or less mobile species (Lovely and Coates, 1997). As a result, the objective of this project is to evaluate and optimize an innovative approach to treat a variety of inorganic and organic oxidized contaminants in a single process that does not produce a residual stream requiring special handling. The innovative process is the hydrogen-based membrane biofilm reactor (MBfR).

The MBfR makes it practical, for the first time, to use H_2 as an electron donor for microbially catalyzed reductions of oxidized contaminants. In the MBfR, H_2 gas is supplied to the inside of special hollow-fiber membranes. The H_2 gas diffuses through the membrane and is consumed almost immediately after it emerges on the outside by a biofilm that naturally coats the outside wall of the membrane. The bacteria in the biofilm gain energy by oxidizing H_2 coming from inside the membrane and one or more oxidized contaminants coming from the water. Thus, the membrane wall is the meeting place of the bacteria's electron donor and electron acceptor, and it is where the bacteria naturally accumulate as a biofilm. Supplying H_2 by diffusion, below the bubble-point of the membrane, eliminates the possibility of forming H_2 bubbles and a combustible atmosphere, which prevents using hydrogen gas in other process configurations. Additionally, H_2 is the best electron donor for fueling microbial reductions, because it is the least expensive electron donor, is non-toxic to humans, leaves no residual in the water, and is consistent with society's long-term sustainability goal of moving to a hydrogen-based fuel economy (Ergas and Reuss, 2001; Lee and Rittmann, 2002; Nerenberg et al., 2002).

CONTAMINANTS

Several oxidized contaminants and volatile organic compounds have emerged as drinking water pollutants, including chromate (CrO_4^-), selenate (SeO_4^{2-}), chloroform (CF), trichloroethene (TCE) and 1,1,1 trichloroethane (TCA). Conventional water treatment techniques are not effective in removing these compounds. Advanced treatment techniques, such as reverse osmosis, ion exchange, membrane filtration, and electrodialysis, are effective, but significantly expensive and generate concentrated wastes that require subsequent disposal. Biological reduction may provide a suitable treatment alternative, and the MBfR is the ideal biological

reactor configuration, particularly since H_2 serves as a biologically available electron donor for the reduction of many oxidized contaminants (Rittmann and McCarty, 2001; NRC, 2000).

Chromate

The widespread use of chromate in industries such as leather tanning, metallurgy, electroplating, petroleum refining, textile manufacturing and pulp production has resulted in large quantities of chromium being discharged into the environment (Barnhart, 1997). In the natural environments, chromium is found in trivalent (Cr(III)) and hexavalent (Cr(VI)) forms. Of these, Cr(III) has relatively low toxicity and tends to form insoluble complexes with hydroxides at neutral pH. Thus, it is nearly immobile in the environment (Anderson and Kozlovsky, 1995; Palmer and Wittbrodt, 1991; Davis et al., 1993). On the other hand, Cr(VI) is highly soluble and is, therefore, mobile and bio-available in aquatic systems (Dragun, 1988). At relatively high exposure levels, Cr(VI) compounds are potent irritants whose acute effects include ulceration of skin, eyes, mucous membranes, and the gastrointestinal tract. At low concentrations, typical of those found in the environment, the chronic effects of Cr(VI) are insidious, as Cr(VI) has mutagenic and carcinogenic effects (DeLeo and Ehrlich, 1994; National Toxicology Program, 1991, US Environmental Protection Agency, 1992). The maximum contaminant level for total chromium in drinking water is 0.1 mg/L.

Cr(VI) is reduced under aerobic (Bopp and Ehrlich, 1987; Gopalan and Veeramani, 1994) and anaerobic conditions (Lovley, 1993; Wang et al. 1989), and some Cr(VI)-reducing bacteria can use hydrogen as an electron donor (Marsh and McInerney, 2001). Reduction of chromate has not been shown to stimulate biological growth (Cervantes, 1991). However, direct reduction of Cr(VI) (i.e., in the absence of sulfate reduction) correlated with nitrate reduction by a nitrate-reducing consortium, when straw of cattail was used as organic carbon sources (Vainshtein et al., 2003). The addition of molasses and nitrate to a microcosm was also found to stimulate chromate reduction (Oliver et al., 2003). Chen and Hao (1996) reported that environmental factors including pH, temperature and other electron acceptor that affect the Cr(VI) reduction capability were quantified in the anaerobically enriched mixed culture. If growth with chromate were possible, the yields would be low since chromate reduction provides less free energy per electron than sulfate. If biologically reduced and precipitated, Cr(III) presumably could be removed by filtration.

Selenate

Selenium is widely used in a variety of industries including production of glass, pigments, pesticides, stainless steel, and photoelectric cells (Haygarth, 1994). Selenium is a naturally occurring element of considerable biological interest because of the small difference between concentrations that are physiologically essential and concentrations that are toxic to organisms (Doran, 1982). Selenium is found commonly in four inorganic oxidation states. Se(VI), the most oxidized form of selenium, and Se(IV) are highly water soluble and toxic to biological systems at relatively low concentrations. Elemental Se^0 is highly insoluble in water and therefore has minimum toxicity. The most reduced form of selenium is selenide Se(-II), which may be a highly toxic gas, but is seldom a biological threat because it is readily oxidized to insoluble elemental selenium in the presence of air. The maximum contaminant level for drinking water is 0.05 mg/L total selenium.

Selenium can be reduced to selenite or elemental selenium by bacteria that also use an alternate electron acceptor (Fujita et al., 1997; Rege et al., 1999). For example, selenate was removed concurrently with nitrate by a denitrifying consortia or pure cultures (Macy et al., 1993; Rege et al., 1999; Kashiwa et al., 2000). Some of the bacteria are facultative anaerobes (Fujita et al., 1997). Selenite is more readily reduced than selenate, and numerous microorganisms capable of reducing selenite to elemental selenium have been described (Doran, 1982; Maiers et al., 1988). Little is known, however, about microorganisms capable of reducing selenate to selenite and/or elemental selenium. In all cases, the reduction was dissimilatory, or supported growth. Elemental selenium is insoluble and can be removed by filtration or centrifugation.

Chlorinated Compounds

The contamination of groundwater sources by chlorinated solvents is a widespread problem throughout the United States. Organo-halogen compounds are ubiquitous. They are found in innumerous everyday materials (e.g., PVC), clothing (e.g., Gortex), pharmaceuticals (e.g., vancomycin), and even toothpaste (e.g., tricosan). Soil has significant organo-chlorine content, the ocean is a net source for diverse volatile and semi-volatile compounds, and the atmosphere is a large reservoir. The high anthropogenic production of organo-halogens to meet industrial and consumer demands has resulted in the substantial release of these compounds into the environment (Table 1.1)

Table 1.1 Production of the top industrial chlorinated aliphatic hydrocarbons in the United States (Häggblöm and Bossert, 2003)

Compound	Annual production ($x10^6$ kg)	Primary use
1,2-Dichloroethane	8140	Production of Vinyl chloride, solvent
Vinyl chloride	6235	Production of PVC and synthesis of chlorinated solvents
Chloromethane	385	Production of silicones
Chloroform	215	Manufacture of HCFC-22 (chlorodifluoromethane) and solvents
1,1,1-Trichloroethane	205	Solvents and dry cleaning
Dichloromethane	160	Solvents and paint remover
Trichloroethene	140	Solvents and dry cleaning
Tetrachloroethene	125	Solvents and dry cleaning
Chloroethane	70	Production of ethylcellulose

Chloroform

Chlorinated aliphatic hydrocarbons are common water pollutants and pose a great threat to public health as suspected carcinogens. An important compound from this group is chloroform (CF), which is present in ground water, drinking water, and wastewater. Chlorination of drinking water containing organic matter leads to the formation of CF and other chlorinated

hydrocarbons. CF is also commonly used as an industrial solvent and appears on the priority pollutant list of the U.S. Environmental Protection Agency.

Among the aerobic microorganisms, CF has been shown to be degradable only by methanotrophic bacteria (Alvarez-Cohen et al., 1992; Bouwer et al., 1981; Oldenhuis et al., 1989), ammonia-oxidizing organisms (Vannelli et al. 1990), and a recombinant pseudomonad expressing soluble methane monooxygenase (Jahng and Wood, 1994). Consequently, CF is usually not treated in an aerobic bioreactor and appears in the effluent from conventional wastewater facilities (Namkung and Rittmann, 1987). Some of it is stripped to the atmosphere during aeration. However, in methanotrophic cultures, chloroform and methane compete for the reaction site, soluble methane monooxygenase, decreasing the reaction rate of each (Oldenhuis et al., 1989; Oldenhuis et al., 1991; Spetiel and Leonard, 1992). Furthermore, the requirement for dissolved oxygen and methane may impose practical and economical limitations on aerobic degradation.

Anaerobic conditions may provide an alternative to aerobic systems for chloroform degradation. CF can be degraded anaerobically to dichloromethane (DCM) and chloromethane (CM) by methanogenic enrichment cultures and pure methanogenic cultures (Bouwer and McCarty, 1983; Egli et al., 1987; Gossett, 1985; Krone et al., 1989; Mikesell and Boyd, 1990) and also by non-methanogenic anaerobic cultures (Egli et al., 1990, Fathepure and Tiedje, 1994; Gälli and McCarty, 1989). Several researchers have shown that, at low concentrations, CF can be anaerobically degraded by methanogenic consortia in the presence of a primary substrate such as acetic acid.

Trichloroethene

The chlorinated solvent trichloroethene (TCE) has been widely used as a dry-cleaning agent and for military, commercial, and industrial applications (Gossett and Zinder, 1996; Bradley, 2000). This widespread use, along with their improper handling, storage, and disposal, has resulted in frequent detection in groundwater (Westrick et al., 1984; Mackay and Cherry, 1989). Concerns over the presence of TCE in soil and groundwater have arisen primarily because of the utilization of groundwater as a source of drinking water in a number of areas and the adverse effects of TCE on human health. TCE has the potential to cause liver damage, as well as malfunctions in the central nervous system (Aviado et al., 1976; USEPA, 1995). Since TCE is considered toxic and has drinking water maximum contaminant levels (MCL) of 5 μg/L (Bradley, 2000), much effort, time, and money have been dedicated to cleaning up contaminated sources.

In 1985, aerobic co-metabolic degradation of TCE was demonstrated in soil columns supplied with natural gas and oxygen (Wilson and Wilson, 1985). Since that discovery, many other examples of co-metabolic TCE degradation have been illustrated (Alvarez-Cohen and McCarty, 1991; Smith and McCarty, 1997; Ensign et al., 1992; Chang and Alvarez-Cohen, 1995). Aerobic co-metabolic TCE degradation has also been successful in the field (Hopkins and McCarty, 1995; Hopkins et al., 1993). The lesser chlorinated ethenes -- cis-1,2-dichloroethene (cis-1,2-DCE), trans-1,2-dichloroethene (trans-1,2-DCE) and vinyl chloride (VC) -- can be co-metabolically degraded (Ensign et al., 1992; Koziollek et al., 1999; Dolan and McCarty, 1995; Freedman and Herz, 1996) or used as substrates for growth (Verce et al., 2000; Coleman et al., 2002a; Coleman et al., 2002b) under aerobic conditions. Due to the restrictive conditions needed for co-metabilism, it has not been widely implemented in practice.

A more general and more important mechanism for the removal of TCE in anaerobic aquifers is reductive dechlorination (Bradley, 2000; Ellis et al., 2000; Sherwood et al., 2001; Major et al., 2002; Lendvay et al., 2003). TCE degradation under methanogenic and sulfate-reducing conditions in laboratory (Vogel et al., 1987) and field studies (Semprini et al., 1995; Major et al., 1991; Buscheck et al., 1997; Kästner, 1991; McCarty and Wilson, 1992) has been reported. Anaerobic TCE degradation occurs by reductive dechlorination, a reaction in which hydrogen atoms sequentially replace chlorine substituents. Thus, in the commonly observed TCE transformation pathway, TCE is sequentially reduced to the dichloroethene (DCE) isomers, vinyl chloride (VC), and ethene (Freedman and Gossett, 1989; DiStefano et al., 1991)

1,1,1-Trichloroethane

1,1,1-Trichloroethane (TCA) is a synthetic organic solvent widely used in industrial processes and is a major environmental pollutant commonly found in soil (USEPA, 1991), ground water (Westrick et al., 1984), and the atmosphere (Montzka et al., 2000). TCA is present in at least 696 of the 1430 National Priorities List sites identified by the U.S. Environmental Protection Agency (EPA) (USEPA, 1991). Because of TCA's adverse effects on human health, the EPA has set a maximum contaminant level of 200 μg/L in drinking water (Federal Register, 1989). Even when released to soil or leached to groundwater, the primary environmental fate of TCA is volatilization to the atmosphere, where it interacts with ozone and contributes to the erosion of the ozone layer (USEPA, 1991). TCA is often a co-contaminant in aquifers with chlorinated ethenes, especially tetrachloroethene (PCE) and trichloroethene (TCE), because they have similar industrial uses. Although *in situ* bioremediation processes for the chloroethenes are known (Lee et al., 1998), TCA remediation remains problematic and can prevent site restoration.

TCA undergoes slow abiotic degradation to acetic acid and 1,1-dichloroethene, an EPA priority pollutant (McNab and Narasimhan, 1994).

Biotransformation of TCA has been observed under aerobic and anaerobic conditions in co-metabolic processes (Kim et al., 2000; Aziz et al., 1999; Adamson and Parkin, 1999; de Best et al., 1997). TCA can be degraded by biological and chemical transformations, primarily under anaerobic or reducing conditions (Bouwer et al., 1983; Parson et al., 1985). McCarty and co-workers extensively studied TCA transformations, and, as early as 1987, Vogel and McCarty (1987) proposed pathways of TCA degradation under methanogenic conditions, in which TCA can be biotransformed by reductive dehalogenation to 1,1-dichloroethane (1,1-DCA) and chloroethane (CA). Wrenn and Rittmann (1995, 1996) extensively studied the kinetics of reductive dechlorination of TCA in biofilm reactors active in methanogenesis and sulfate reduction.

Inhibitory Effects on Dechlorination

Since many contaminated groundwater often contain mixtures of chlorinated solvents, a better understanding of co-contaminant effects is needed for the selection of appropriate treatment strategies. 1,1,1-TCA (Erasin et al., 1994) and especially CF (Chidthaisong and Cornard, 2000) are known to inhibit methanogenesis and may also interfere with reductive dechlorination (Bagley et al., 2000; Maymo-Gatell, 2001). CF may become an inhibitor under the dechlorination of chlorinated solvents (Duhamel et al., 2002) and was shown to inhibit reductive dechlorination of cis-1,2-DCE and VC at concentrations as low as 77 μg/L (Maymo-Gatell,

2001). CF has been observed to inhibit its own degradation and acetate consumption at approximately 330 µg/L under perhaps methanogenic conditions, and the inhibition appears to be less under sulfate-reducing conditions at a concentration of approximately 2 mg/L (Gupta et al., 1996). Others report that CF can inhibit unacclimated cultures at very low concentrations of CF can be tolerated and there is a direct relation between CF concentration and inhibition (Stickley, 1970; Narayan et al., 1993; Yang and Speece, 1986).

RESEARCH APPROACH

The primary objectives of this project were to evaluate and optimize an innovative process (the MBfR) to treat inorganic and organic oxidized contaminants impacting groundwater supplies around the country and abroad. In support of these objectives, the following project goals outline the major tasks of the project:

- Bench-Scale Experiments on Biological Reduction Fundamentals. Conduct fundamental bench-scale experiments to systematically evaluate the potential of the MBfR to remove a variety of oxidized inorganic and organic compounds and understand the micro-ecology behind these systems.
- Influence of Hydraulics. Develop a hydrodynamic model of the existing MBfR to aid in identifying how the hydraulics of the reactor (flow rates, membrane fiber orientation, influent/effluent configurations, etc) can be used to optimize the system (biofilm thickness, microecology, mass transport, etc).
- Regulatory Approval. Document and identify the specific requirements that need to be satisfactorily addressed for obtaining CaDHS approval of MBfR process for the production of potable water.

CHAPTER 2

BENCH-SCALE MATERIALS AND METHODS

EXPERIMENTAL SET-UP

A schematic of the MBfRs used in this study is shown in Figure 2.1, and the physical characteristics of the reactors are provided in Table 2.1. Each MBfR system consisted of two glass tubes (each 25-cm long) connected with Norprene tubing and plastic barbed fittings. One glass tube contained a main bundle of 32 hollow-fiber membranes (Model MHF 200TL, Mitsubishi Rayon). In order to take biofilm samples from a MBfR without disturbing the main bundle of fibers and causing a significant change of surface area in the reactor, the other tube contained a single fiber. The high recirculation rate of each reactor (150 mL/min) promoted completely mixed conditions and helped control biomass accumulation on the fibers. Another advantage of a high recirculation rate was the high hydraulic shear on the fibers, which provided a dense biofilm (Chang et al. 1991) and minimized the accumulation of excessive biofilm that might clog the reactor.

Table 2.1 Physical characteristics of MBfRs

	Units	Main Tube	Coupon Tube	Reactor total
Tube inside diameter	cm	0.6	0.5	-
Number of hollow fibers		32	1	33
Cross-sectional area fibers	cm^2	0.0197	0.0006	0.0203
Feed rate	mL/min	-	-	1
Recirculation rate	mL/min	-	-	150
Net cross sectional area	cm^2	0.26	0.20	-
Fiber surface area	cm^2	70.4	2.2	72.6
Liquid velocity	cm/min	570.3	766.3	-
Average hydraulic detention time	min	-	-	23.9

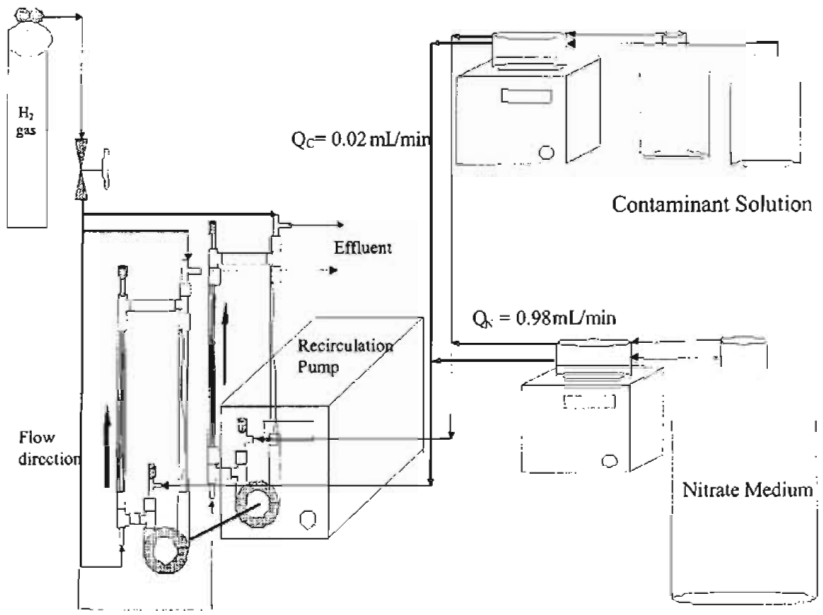

Figure 2.1 Schematics of the bench-scale MBfRs

STANDARD OPERATING CONDITIONS

A single peristaltic manifold was used to give a nitrate-medium-feed rate of 0.98 mL/min. A second manifold pump supplied the chlorinated solvents stock solution at rate of 0.02 mL/min into the feed line from the nitrate medium, thereby giving a total feed flow rate of 1 mL/min. The recirculation rate was 150 mL/min, giving a recirculation ratio of 150. The standard hydrogen pressure for both reactors was 2.5 psi (0.17 atm).

Solutions

The nitrate medium, described in Table 2.2, was prepared in an 8-L glass bottle (Pyrex) and filter sterilized into another sterile 8-L glass bottle using a capsule filter (Pall SuporCap 100, Pall Corporation, Ann Arbor, MI). The two stock solutions contained deionized water with 50 mg/L of Cr(VI) (from K_2CrO_4) or Se(VI) (from Na_2SeO_3). When the nitrate-medium and the chromate or selenate stock solutions were mixed, the influent concentrations were 5 mg NO_3^--N/L and 1,000 μg/L as Cr or Se over the experimental period of 92 days. In order to determine the effect of Cr or Se loading, the influent concentration of chromate or selenate was reduced to 250 μg/L in the presence of the same concentration of nitrate.

The two mixed chlorinated solvents stock solutions contained deionized water with 50 mg/L each of TCF, TCE, and TCA. When the nitrate-medium and the chlorinated solvents stock solutions were mixed, the influent concentrations were 5 mg NO_3^--N/L and 1,000 μg/L of CF, TCE, and TCA over the experimental period. In order to determine the effect of chlorinated solvents loading, the influent concentration of chlorinated solvents was increased to 2,500 μg/L in the presence of the same concentration of nitrate after 51 days of operation.

Table 2.2 Medium and trace mineral solution

Nitrate Medium (per liter)		
KH_2PO_4		0.128 g
Na_2HPO_4		0.434 g
$MgSO_4 \cdot 7H_2O$		0.2 g
Nitrate stock (10 g-N/L)		0.5 mL
$CaCl_2 \cdot 2H_2O$		0.001 g
$FeSO_4 \cdot 7H_2O$		0.001 g
Trace mineral solution		1 mL
• $ZnSO_4 \cdot 7H_2O$	100 mg/L	
• $MnCl_2 \cdot 4H_2O$	30 mg/L	
• H_3BO_3	300 mg/L	
• $CoCl_2 \cdot 6H_2O$	200 mg/L	
• $CuCl_2 \cdot 2H_2O$	10 mg/L	
• $NiCl_2 \cdot 6H_2O$	10 mg/L	
• $Na_2MoO_4 \cdot 2H_2O$	30 mg/L	
• Na_2SeO_3	30 mg/L	

Inoculation and Start Up

The inoculum was obtained from the pilot-scale MBfR operated by MWH at La Puente, California (Nerenberg 2003). The pilot-scale reactor treated groundwater with approximately 5 mg-N/L of nitrate and 60 µg/L of perchlorate. It had two modules in series; most of the nitrate was removed in the first module, and most of the perchlorate in the second. Biofilm samples were taken from first and second modules and mixed together. This mixture was added to a sterile glycerol solution with a final concentration of 25 percent glycerol. For inoculating the Cr- and Se-reducing MBfRs, biofilm samples were washed twice by centrifuging for 15 min at 5,000 g and resuspending it in 10-mL of sterile minimal medium without electron donor. A 1.5-mL aliquot of the washed biofilm suspension was added into each reactor.

Start-up began when H_2 gas was supplied and the liquid in the reactor was recirculated for 24 hours to establish a biofilm. Initially, influent medium containing only nitrate was fed at a rate of 0.2 mL/min to each reactor. The concentration of nitrate in the effluent reached steady state after 3 days, and then the feed rate of influent medium was increased to 1.0 mL/min. After nitrate was completely removed (approximately 20 days), chromate or selenate was added to the influent of each reactor.

ANALYSIS

The performance of the reactors was monitored by analyzing influent and effluent samples for selected parameters according to standard procedures. Samples were taken and analyzed on a daily basis and immediately filtered through a 0.2-μm membrane filter (Pall Corp., Ann Arbor, ML). After sample centrifugation (15,000 g, 10 min), total soluble selenium (Se(IV) + Se(VI)) and chromium (Cr(III) + Cr(VI)) were determined by ICP-MS (PQExCell, VG Elemental). In order to investigate the degree of reduction of oxidized contaminants, Se(IV) and Cr(VI) concentrations were analyzed by a fluorometric method for Se(IV) (Standard method 3500-Se E) and diphenyl carbazide method (3500-Cr D) for Cr(VI). The Cr(III) concentration was determined by subtracting Cr VI) from total chromium. The concentration of Se(VI) was calculated by subtracting Se(IV) from total Se in the effluent. This approach assumes that selenium reduced to Se^0 results in a solid that is removed by centrifugation. The concentration of selenium removed as Se^0 was computed as the difference between influent and effluent total Se. Analyses for nitrate and nitrite are carried out by ion chromatography using an AS-11 column, an AG-11 pre-column, and a 200-μg/L injection loop, as described in Nerenberg et al. (2002).

The sulfate concentration was measured using a capillary ion analyzer (Millipore Corp., Milford, MA), and the dissolved sulfide concentration in the aqueous phase was measured using a colorimetric method based on methylene blue formation (Cline, 1969).

A headspace-analysis method (Schmidt and Ahring, 1993) was used for the dissolved H_2. A 1-mL liquid sample was transferred from the reactor to a 160-mL serum vial previously out-gassed with N_2. The vials were shaken vigorously to liberate the dissolved H_2. A gas-tight syringe was used to sample the headspace (1 mL) and test for hydrogen by the reduction gas analysis (RGA3, Trace Analytical, Menlo Park, CA). In this method, H_2 is directed through a HgO bed and produces Hg (g), which is measured by an ultraviolet photometer. Once the H_2 concentration is known in the gas, Henry's law and mass balance are used to determine the H_2 concentration in the liquid sample.

The volatile organic compounds (VOCs) -- chloroform (CF), dichloromethane (DCM), chloromethane (CM), trichloroethene (TCE), cis-1,2-dichloroethene (cis-1,2-DCE), trans-1,2-dichloroethene (trans-1,2-DCE), 1,1-dichloroethene (1,1-DCE), vinyl chloride (VC), 1,1,1-trichloethane (TCA), 1,1-dichloroehane (DCA) and chloroethane (CA) -- were routinely determined by gas chromatographic (GC) analysis. A 0.5-mL headspace sample was analyzed by a GC (HP 5890) with a Rtx-503.2 capillary column (20 m x 0.18 mm x 1.00 μm, Restek, Bellefonte, Pa), a flame ionization detector (FID), and solid-phase micro-extraction (SPME) fiber assortment (Supelco). The conditions of the GC were the following: initial temperature of 40°C held for 2 min, and a temperature program with an increment of 25°C/min to 115°C, and then 10°C/min until 250°C, which was held for 3 min. Detection limits were at or near 10 μg/L for all compounds. GC calibration factors were measured to relate directly the total mass of compound present in a serum bottle to the GC peak area obtained from a 0.5-mL headspace injection. Known masses of CF, TCE, cis-1,2-DCE, trans-1,2-DCE, 1,1-DCE, TCA, DCA, and CA were added to replicate serum bottles containing 100 ml of distilled deionized water, allowed to equilibrate at 40°C, and then analyzed by GC. Standard additions of DCM, CM, and VC were

produced from gaseous stocks. Coefficients of variation [(standard deviation mean) x 100%] for the calibration factors ranged from 0.63 to 2.5%.

Methane, ethane, and ethane were quantified by GC, using the same column and detector conditions as for the chlorinated compounds, but with direct injection of gaseous samples. Liquid samples (1 mL) were placed into 2-ml vials and sealed with Teflon-lined silicon septa. After equilibration with agitation at 25°C for 20 min, a 10-μL headspace sample was removed and injected directly onto the GC for quantification. The oven temperature was set to 120°C.

CHAPTER 3

BENCH-SCALE RESULTS

START UP

In the first few days of operation, some nitrate was converted only to nitrite, but the nitrate and nitrite concentrations in the effluent dropped to less than 15 μg-N/L within 10 days. These results are summarized in Figure 3.1 and Figure 3.4.

CHROMATE-REDUCING MBfR

Cr(VI) Reduction

On day 21, chromate was first added to the feed of the Cr-MBfR. Figure 3.1 shows the concentrations of nitrate, nitrite, total chromium, Cr(VI), and the reduced Cr(III) in the effluent from that reactor. The reduction of Cr(VI) to Cr(III) began within the first two days of Cr(VI) addition. Steady-state reduction of Cr(VI) to Cr(III) was evident by day 32, or after 11 days of feeding Cr(VI). The average reduction of Cr(VI) to Cr(III) was 45±6 percent, yielding an effluent Cr(III) concentration of 440±60 μg/L. The effluent concentration of total Cr reached approximately 1,000 μg/L, which indicates that the reduced Cr(III) was not a solid that was removed by centrifugation. Total Cr concentration decreased minimally (<5 μg/L) after filtration using a 0.2-μm membrane filter. Thus, the reduced Cr(III) in the effluent was either soluble or present in colloids smaller than 0.2 μm.

On day 65, the hydrogen pressure was increased to 4.0 psi. The Cr(VI) concentration in the effluent gradually decreased and reached a steady state on day 68, or 10 days after the pressure change. From day 68, the average concentrations of Cr(VI) and Cr(III) in the effluent were 406±35 μg/L and 549±51 μg/L, respectively, and the average reduction of Cr(VI) was 57±4 percent. These results confirm that chromate reduction is controlled by H_2 availability, a situation that holds for reductions of nitrate and perchlorate (Nerenberg et al., 2002; Lee and Rittmann, 2002).

Since Cr(III) reached an apparent steady-state removal for over 10 days (from day 82 to day 92), the influent Cr(VI) loading was changed systematically from day 93 to an initial Cr(VI) concentration of 250 μg/L for assessing kinetic and capacity for eliminating Cr(VI) totally. The Cr(VI) and Cr(III) concentrations in the effluent reached steady state by day 106, or 14 days after the influent loading decreased. From day 106 to day 118, the average level of Cr(III) was 136±16 μg/L, and the average reduction of Cr(VI) was 63±4 percent. This result confirms the expected trend that Cr(VI) reduction is more complete with a lower Cr(VI) loading, but this lower loading did not lead to 100 percent reduction.

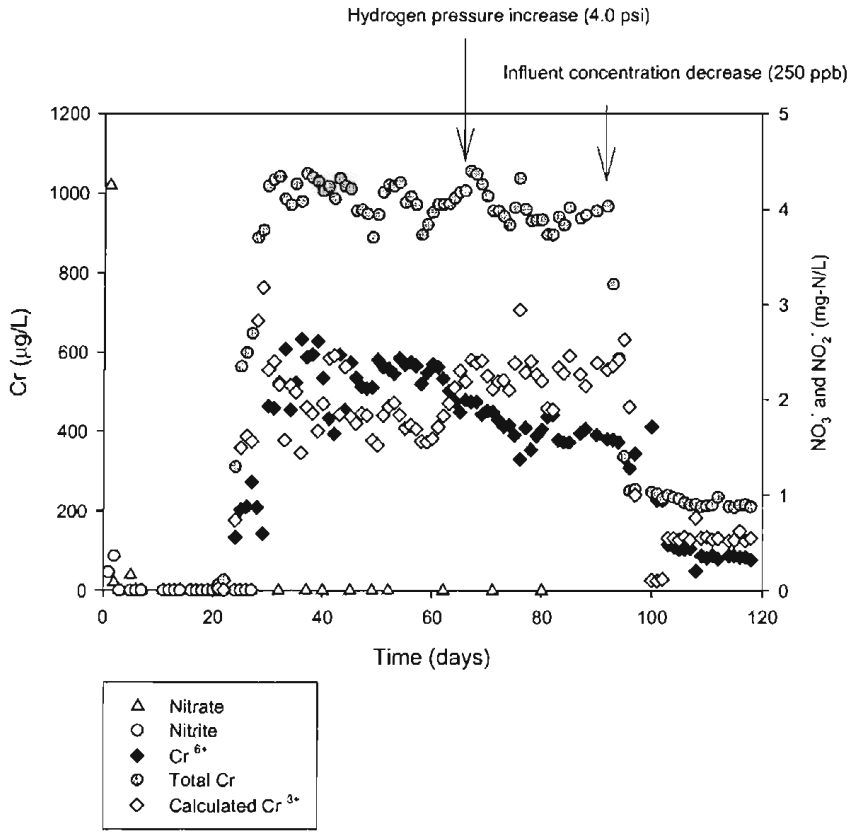

Figure 3.1 Simultaneous nitrate and chromate reduction in the MBfR. The influent had 5 mg/L of NO_3^--N and 1,000 µg/L of CrO_4^{2-}-Cr.

Cr(III) Precipitation

In order to investigate the character and removal potential of the reduced Cr(III), a precipitation test was performed using the effluent from chromate-reducing MBfR. This test is carried out in a well-mixed batch reactor using effluent contained Cr(VI) and Cr(III). First, 0.5-mM hydrochloric acid was added to lower the pH to 3; then, 0.5-mM sodium hydroxide was titrated to increase the pH. The precipitation of $Cr(OH)_3(s)$ was expected with a pH higher than the usual effluent pH of about 7.2, since HO^- is a ligand for $Cr(OH)_3$. At each pH, the pH was held constant for 20-30 minutes. Then, 10-mL of the solution was used for the measurement of optical density by ultraviolet spectrophotometry at 600 nm. The sample was then passed through a 0.2-µm membrane filter, acidified with concentrated nitric acid, and analyzed later by ICP/MS analysis to determine the remaining Cr concentrations.

The test results are shown in Figure 3.2, which shows the remaining dissolved concentration of total chromium after filtration and optical density at 600 nm. Both results show that precipitation of Cr(III) started at a pH of about 7.0, and most was precipitated at pH of 7.5 to 9.0. The solid redissolved at pH $\geq$ 10, probably due to formation of $Cr(OH)_4^-$. These results indicate good potential to remove reduced Cr (III) by small adjustment of the pH.

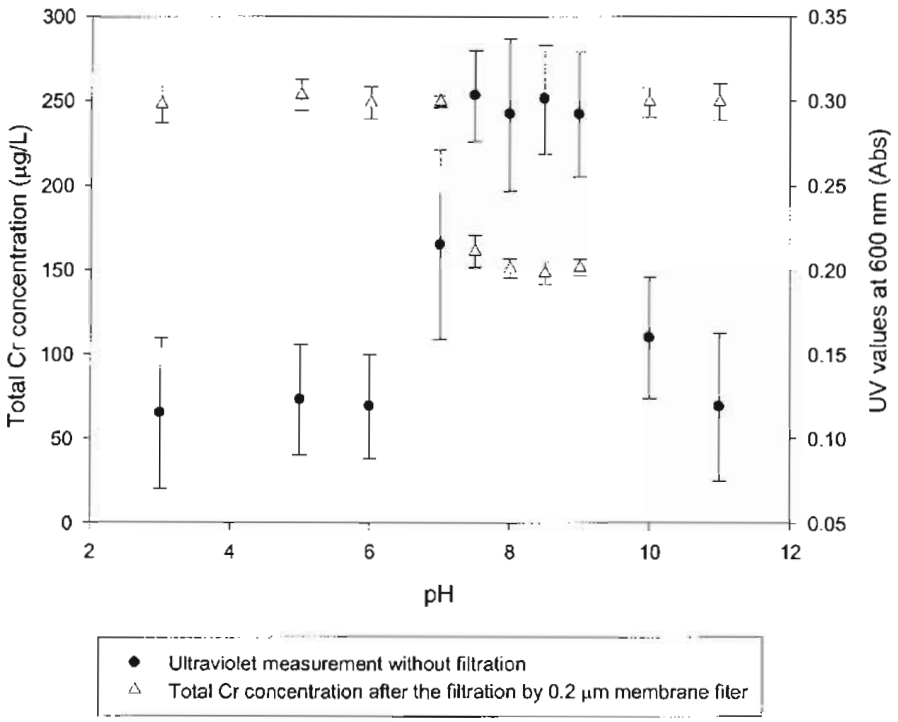

Figure 3.2 Post processing chromium precipitation by pH adjustment

Sulfate Reduction

Sulfate reduction was investigated in the chromate-reducing MBfR. As shown in Figure 3.3, chromate may have inhibited the reduction of sulfate, since almost no sulfide was produced. Although chromate anions have the same charge and a similar physical size to the sulfate anion and also have the potential to enter into sulfate transport pathways in the biological system, this result implies that chromate acts as the inhibitor of sulfate reduction, like molybdate. Generally, molybdate forms unstable analogues of active sulfate, depleting cells of ATP (Postgate, 1984; Smith and Gadd, 2000).

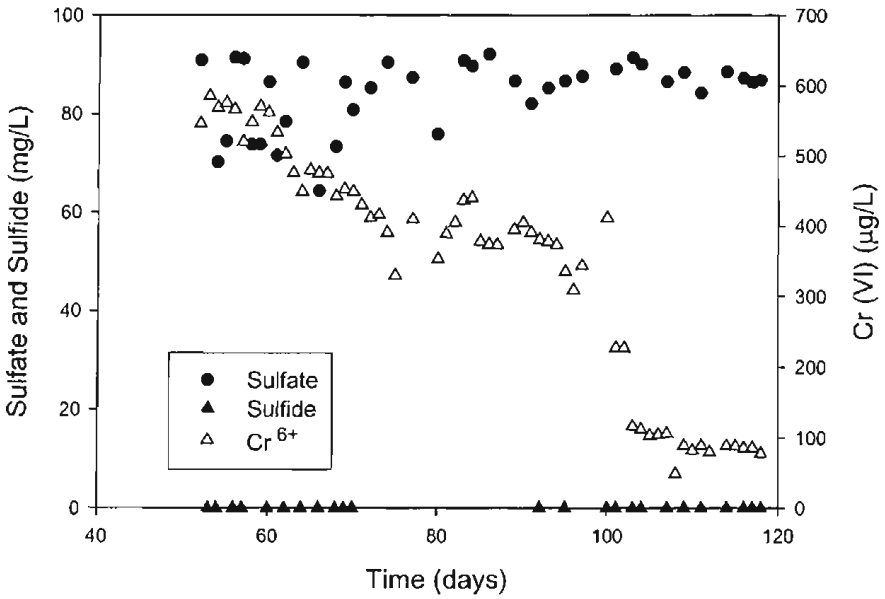

Figure 3.3 Inhibition of sulfate reduction by chromate

SELENATE-REDUCING MBfR

Se(IV) Reduction

Figure 3.4 shows the concentrations of nitrate, nitrite, total selenium, Se(VI), reduced Se(IV), and the reduced elemental selenium (Se^0) in the effluent from selenate-reducing MBfR. Se(VI) was reduced to Se(IV) within one day of Se(VI) addition. Initially and up to day 38, Se(VI) was reduced exclusively to Se(IV), which is completely soluble. On day 38 (or 13 days after Se(VI) feeding began), Se(IV) began to be removed, most likely due to reduction to Se^0. The maximum removal (587 µg/L) was observed on day 47.

From day 51 to day 64, the average levels of Se(IV), Se(VI), and Se removed as Se^0 were 270±40 µg/L, 87±25 µg/L, and 590±30 µg-Se/L. Thus, the average removal of Se was about 59 percent within this period shown in Figure 3.4, but the reduction of Se(VI) was about 72 percent.

The H_2 pressure was changed to 4.0 psi from day 65 in order to improve the capacity of reduction. More complete steady-state reduction of Se(VI) to Se(IV) and Se^0 was evident by day 81. From day 82 to day 92, the average levels of Se(IV) and Se removed as Se^0 were 135±8 µg/L and 810±5 µg-Se/L, respectively. The average removal of Se in this period was about 83 percent. This trend, similar to the Cr-MBfR, again shows that the availability of H_2 gas controls the reduction kinetics.

Once Se(VI)-removal reached a steady state, the influent Se(VI) loading was changed to the new initial concentration of 250 µg/L for evaluating the kinetics and capacity for Se(VI) reduction after day 93. Clearly, selenate and selenite were easily reduced to solid-state selenium if the selenate loading was not too high. Furthermore, Se^0 could be removed within the MBfR. The

calculated Se(VI), Se(IV), calculated elemental selenium concentrations in effluent and average selenium removal rate were summarized in Table 3.1.

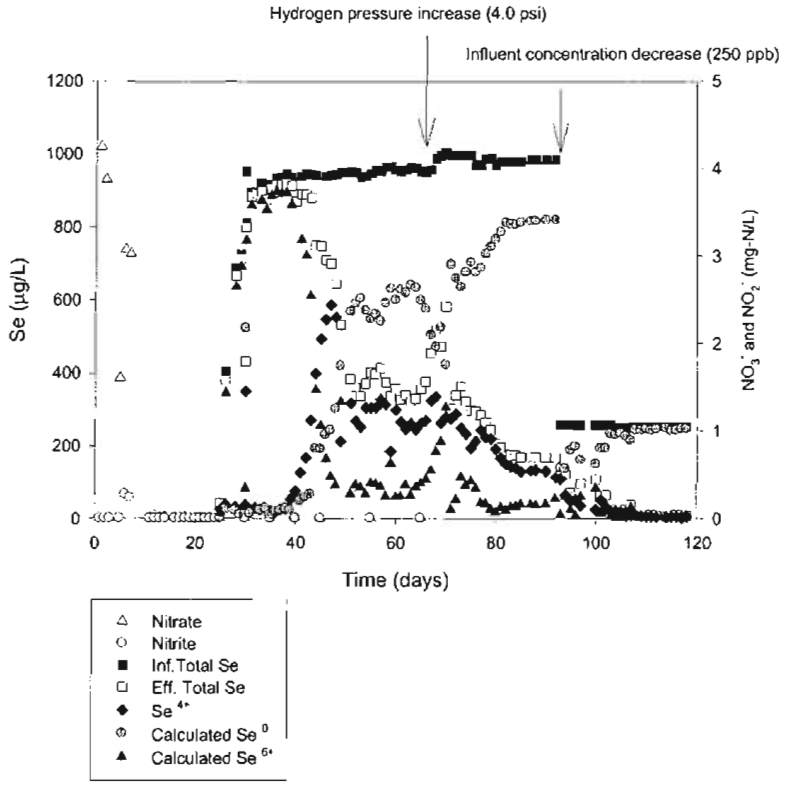

Figure 3.4 Simultaneous nitrate and selenate reduction in the MBfR. Influent concentration were 5 mg/L of NO_3^--N and 1,000 µg/L of SeO_4^{2-} as Se.

Table 3.1 Selenate reduction summary

Steady-state period (day)	51-64	82-92	106-118
H_2 pressure (psi)	2.5	4.0	2.5
Influent concentration of Se (µg-Se/L)	1,000	1,000	250
Se(VI)	87±25 µg/L	55±4 µg/L	7.2±6.1 µg/L
Calculated Se(IV)	270±40 µg/L	135±8 µg/L	4.4±1.9 µg/L
Se removed as Se^0	590±30 µg-Se/L	810±5 µg-Se/L	245±6 µg-Se/L
Average removal of Se	59 %	83%	98%

For the selenate-reducing MBfR, the quantity of Se associated with the effluent suspended solids (SS) versus the biofilm was determined. Addition of hydrogen peroxide (H_2O_2) oxidized Se^0 to soluble forms that were assayed by ICP/MS. First, the suspended solids and dissolved selenium

species in the effluent from the selenate-reducing MBfR were measured. The SS was 0.05±0.01mg-cells/L and dissolved selenium species was 6.8 μg-Se/L. Then, 10 mL of same effluent samples were treated with 1 mL of 10 percent hydrogen peroxide, filtered by 0.2-μm membrane filter, and analyzed by ICP/MS. The dissolved concentration of selenium species was 39.5±0.6 μg-Se/L. This result indicates that the effluent suspended solids were mostly Se^0 (i.e., 39.5/50 = 79%).

Sulfate Reduction

The relationship of sulfate reduction to the reduction of selenate and selenite was investigated for the selenate-reducing MBfR. As shown in Figure 3.5, sulfate reduction occurred over most of the experimental period. Once selenite was reduced completely, sulfide was a significant reduction product. This result shows that selenium species did not inhibit sulfate reduction, at least not at the concentrations present in the experiments. Even through many strains of Se(VI)/Se(IV)-reducing bacteria are able to use sulfate as electron acceptor (Oremland et al., 1989; Lortie et al., 1992), only extremely high levels (500 mg/L as S) of sulfate significantly inhibited selenite reduction (Wan et al., 2001). Losi and Frankenberger (1997) observed sulfate inhibition on selenite reduction when the sulfate inhibition was 230 times higher than selenate. The inhibition of sulfate in the selenate-reducing MBfR probably was caused by competition of H_2.

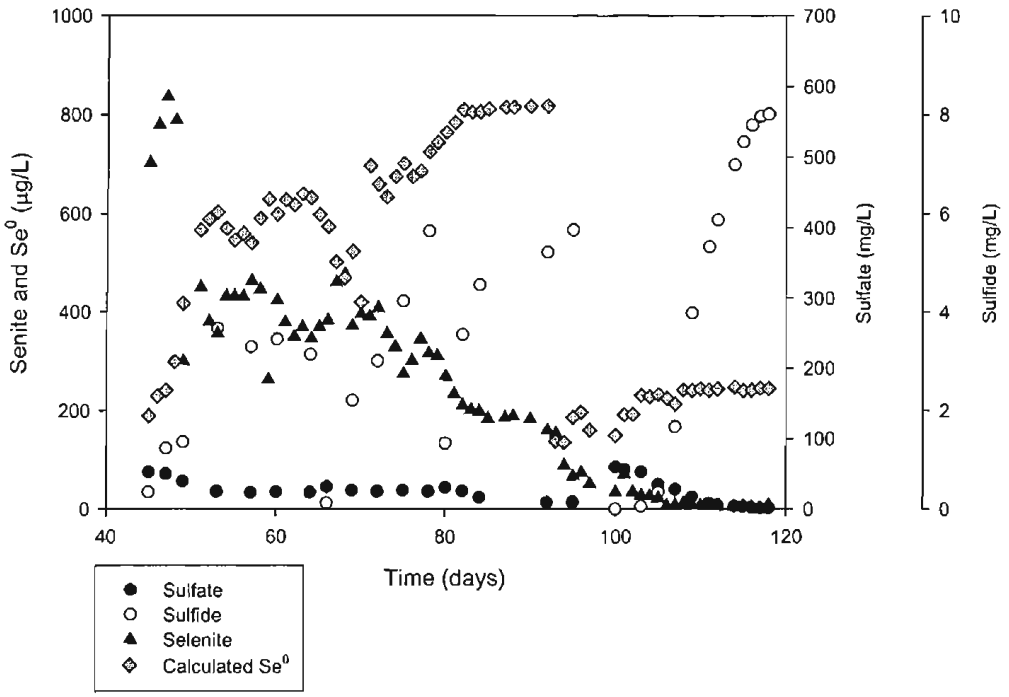

Figure 3.5 Inhibition of selenite reduction by sulfate, but no inhibition of sulfate reduction by selenate.

MIXED MATRIX EFFECTS

These series of tests were conducted to investigate if and how the hydrogen concentration, chromate concentration, nitrate concentrations, and pH affected chromate or selenate reduction.

Another goal of these experiments was to evaluate a range of concentrations and H_2 pressure. From the results of this testing, the kinetics of selenate and chromate reduction in the MBfRs could be evaluated. The experiments were divided into four series; the conditions are described below in Table 3.2. Prior to the experiments, the reactor was operated to as steady state with an influent with 1 mg/L of chromate and selenate, 5 mg-N/L of nitrate, and a 2.5 psi of hydrogen pressure. The steady-state nitrate removal was 99.8 percent, and the chromate and selenate reductions were approximately 48 percent and 60 percent, respectively.

Table 3.2 System conditions for mixed matrix evaluation

Series Number	H_2 pressure (psi)	Influent Concentration		Influent pH
		Chromate or Selenate (μg/L)	Nitrate (μg-N/L)	
Series #1	2.5	1,000 500 250 100	5,000	7.5
Series #2	2.5 4.0 5.5	1,000	5,000	7.5
Series #3	2.5	1,000	10,000 5,000 2,500 1,000 0	7.5
Series #4	2.5	1,000	5,000	6.5 7.1 7.6 8.2 8.9

The tests were conducted with three H_2 pressures, each of which had four different chromate and selenate concentrations. Then, the nitrate concentration of the influent was varied to test for hydrogen competition between nitrate and chromate or selenate reduction. Finally, the pH of the influent was varied to test for pH effects on the efficiency of chromate reduction.

A series of measurements for steady-state effluent quality was conducted over three days before the tests began. For each test, the change of system conditions lasted for two hours before samples were taken. With a liquid retention time of 23.9 minutes in the MBfR, two hours (more than 5 liquid retention times) were long enough for the system to reach a pseudo-steady-state,

which is defined as a condition in which the liquid concentration reached a stable state, while the biofilm accumulation and biomass were not changed significantly from the true steady state, due to the short duration of the change. After each test was completed, the system was changed to the steady state before the next series of tests began.

In the first experiment, the influent chromate or selenate concentration was set to 100, 250, 500, or 1,000 μg/L, with applied hydrogen and influent nitrate at the steady-state values of 2.5 psi (0.17 atm) and 5 mg-N/L, respectively. Results are shown in Figure 3.6. Although nitrate reduction was not affected by the influent chromate or selenate load, the percentage chromate/selenate removal decreased gradually with the increased influent load. For selenate, selenite was detected when the influent selenate was 500 and 1,000 μg/L. Total Se-removal percentages, including selenite, reached 59 percent at the 1,000 μg/L of influent concentration (data not shown).

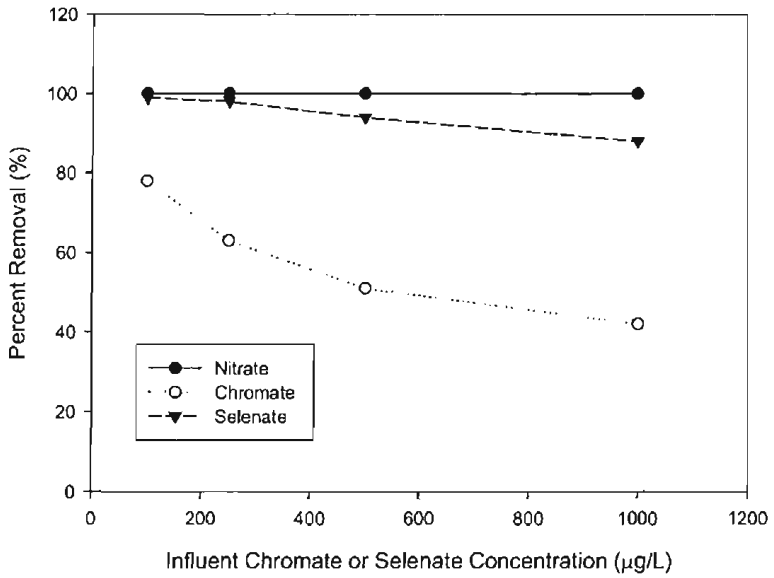

Figure 3.6 Impact of contaminant influent concentration on reduction efficiency

In the second experiment, the applied H_2 pressure was set to 2.5 psi (0.17 atm), 4.0 psi (0.27 atm), and 5.5 psi (0.37 atm). As shown in Figure 3.7, increasing hydrogen pressure gave greater removals of chromate and selenate. At 2.5 psi applied pressure, the effluent residual H_2 was 17 μg/L, and denitrification already had reached its maximum removal of over 99.5 percent. Although nitrate removal did not increase further at higher H_2 pressure, the reductions of chromate and selenate increased by 12 percent and 9 percent, respectively. Increasing the H_2 pressure to 5.5 psi gave a small increase to Cr reduction, but the effluent H_2 concentration rose to $\geq$ 680 μg/L.

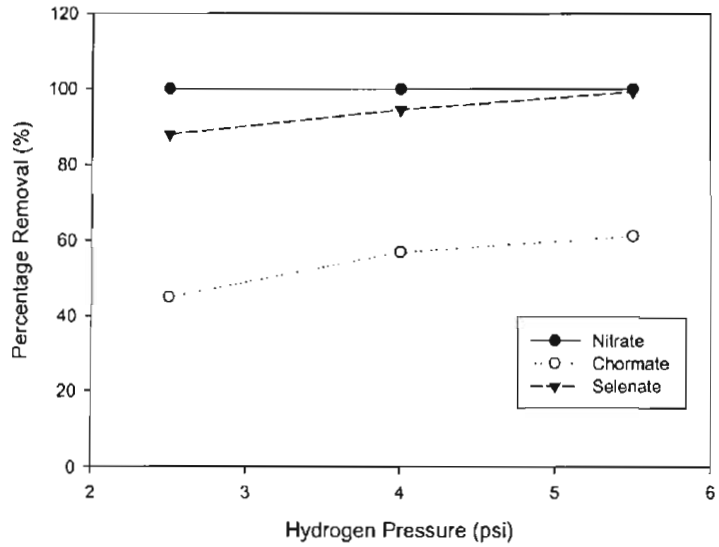

Figure 3.7 Impact of hydrogen pressure on chromate and selenate reduction efficiency

In the third experiment, the nitrate concentration was varied from 0 to 10 mg-N/L, with hydrogen pressure and chromate/selenate concentration at the steady-state levels of 2.5 psi and 1 mg/L, respectively. As shown in Figure 3.8, chromate removal significantly increased, and selenate reduction modestly increased when no nitrate was in the influent. With zero nitrate in the influent, the percentage removals of chromate and selenate increased to 84 percent and 96 percent, respectively. Thus chromate (especially) and selenate reductions were strongly affected by either a very small concentration of nitrate or (more likely) competition of H_2 from nitrate reduction.

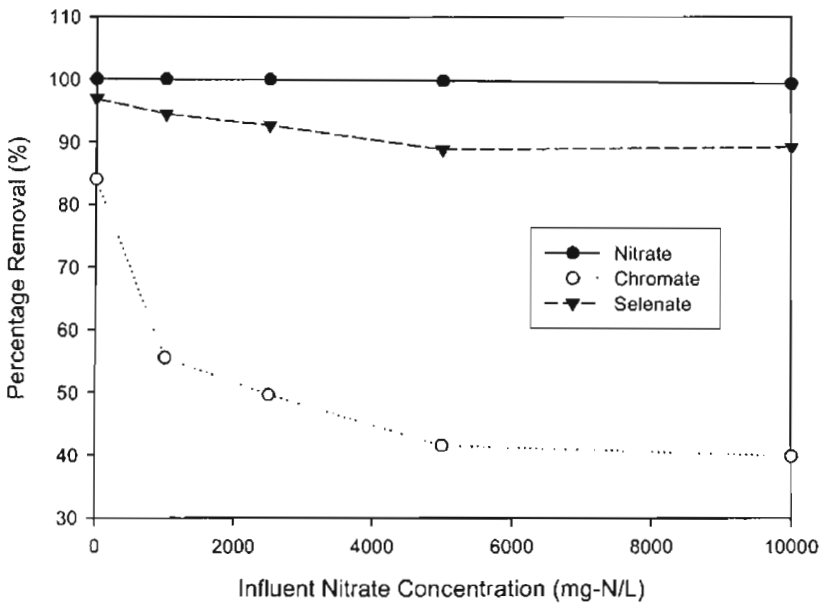

Figure 3.8 Impact of nitrate concentration on chromate and selenate reduction efficiency

In the fourth experiment, the influent pH values were set to 6.5, 7.1, 7.6, 8.2, or 8.9, with applied hydrogen pressure, influent chromate/selenate concentration, and influent nitrate concentration at their steady-state values of 2.5 psi, 1 mg/L, and 5 mg-N/L, respectively. As shown in Figure 3.9, chromate reduction was relatively sensitive to pH. Although nitrate and selenate reduction was hardly sensitive to pH from 7.0 to 9.0, chromate reduction was pH sensitive, with a maximum removal at the pH of around 7.0. The optimal pH for selenate reduction was around 7.5. The fairly sharp pH optimum for chromate reduction may be important, because denitrification adds base, which can cause a pH increase that might slow chromate reduction.

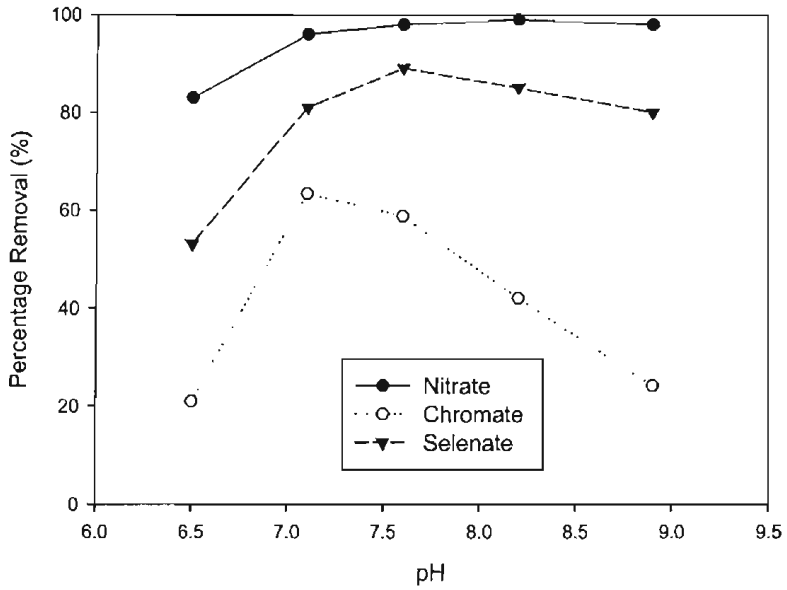

Figure 3.9 Role of pH on contaminant reduction efficiency

SWITCHED FEED EXPERIMENTS

In order to evaluate the reduction capacity of each MBfR for the other oxidized contaminant, chromate was applied to the Se-reducing MBfR and selenate to the Cr-reducing MBfR after day 130. The influent chromate/selenate concentration was 250 μg/L, with applied H_2 pressure and influent nitrate concentration at their steady-state values of 2.5 psi, and 5 mg-N/L, respectively.

Figure 3.10 illustrates the concentrations of selenium species in the effluent from the Cr-reducing MBfR. When Se(VI) feeding began, Se(IV) was reduced immediately to Se^0. On day 16, concentrations of Se(IV) and calculated Se(VI) were below 20 μg/L, and the selenium removed as Se^0 had gradually increased to over 90 percent.

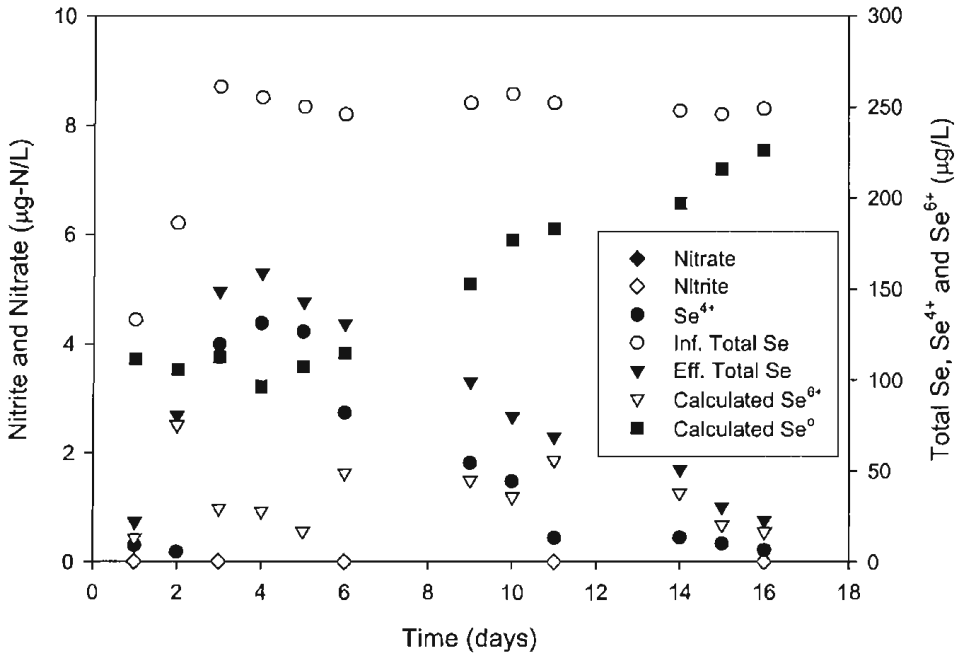

Figure 3.10 Selenium reduction in the chromate-reducing MBfR

Figure 3.11 shows the concentrations of chromium species in the effluent from Se-reducing MBfR. When Cr(VI) feeding began, Cr(VI) was immediately reduced to Cr(III). Most of these Cr(III) species precipitated as hydroxide compounds and could be removed by filtration. From day 10, total chromium in the effluent was below 10 µg/L, and chromium reduction rate in Se-reducing MBfR was higher than that in Cr-reducing MBfR.

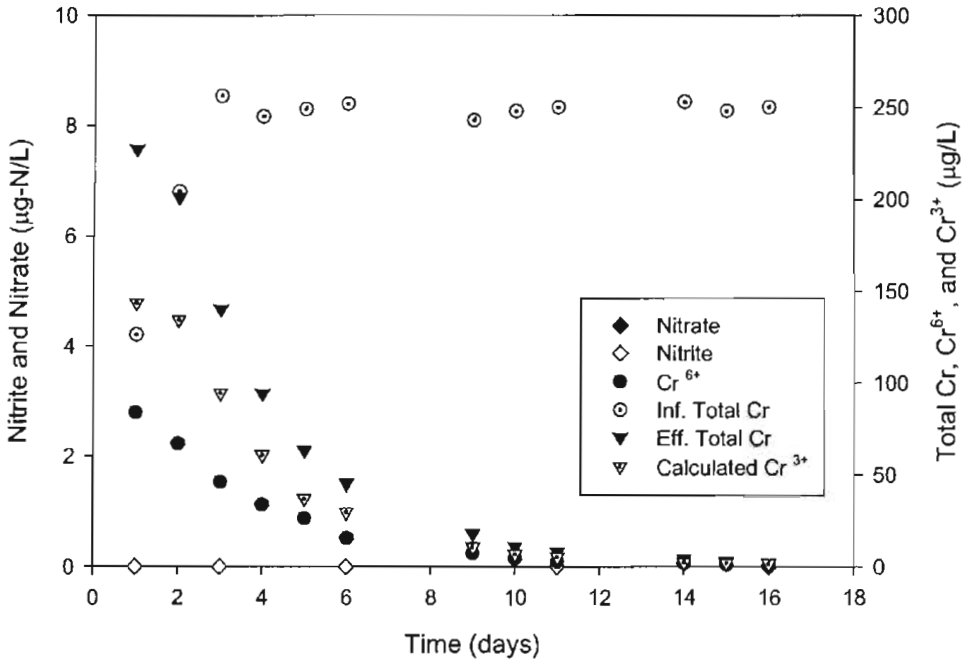

Figure 3.11 Chromate reduction in the selenate-reducing MBfR

CHLORINATED COMPOUNDS

Dechlorination of Chlorinated Solvents

The objective of the first phase of this work was to ascertain whether chlorinated solvents can be dechlorinated in an MBfR using hydrogen as the electron donor delivered to a biofilm by diffusion through the membrane wall. In order to determine the dechlorination rate for each chlorinated solvent without any interfering compounds, such as sulfate and other chlorinated solvents, three MBfRs were operated with three kinds of feed streams (8.4 µM (1 mg/L) CF, 7.6 µM (1 mg/L) TCE, and 7.5 µM (1 mg/L) TCA).

Figure 3.12 shows CF, DCM, and CM concentrations in the effluent when CF was added as the only electron acceptor besides nitrate. After nitrate was completely removed in the effluent from the MBfR, 8.4 µM CF was added to the influent. When CF was added, dechlorination of CF started immediately. The CF concentration in the effluent decreased with time, indicating increasing transformation of CF by the microorganisms. DCM was formed transiently as a result of CF reduction, but was transformed after the CF had completely disappeared. By day 10 after adding CF, CM appeared transiently. After day 10, methane was observed at 0.38 µM, but decreased over time.

These results show that the MBfR was highly active at reductive dechlorination of CF. The less-chlorinated reduction products appeared briefly, but all chlorinated organics were eliminated by day 22. At least some of the original CF appeared as methane. CM is susceptible to hydrolysis, along with reductive dechlorination. Thus, some of the CM could have been hydrolyzed to methanol, which could not be detected.

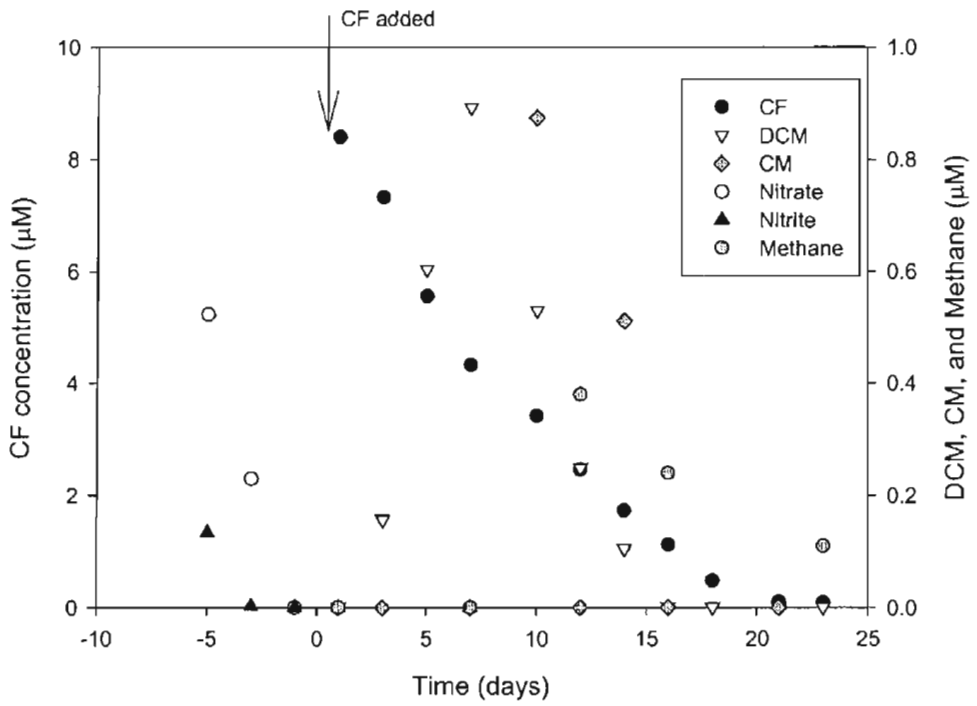

Figure 3.12 CF, DCM, CM, and methane concentrations in the effluent from the CF-dechlorinating MBfR (Left Y-axis: CF concentration (μM); Right Y-axis: DCM, CM, and methane concentration (μM))

Figure 3.13 shows TCE, its intermediates, and ethene concentrations in the effluent when TCE was added as the only electron acceptor besides nitrate. The TCE concentration in the effluent decreased rapidly over 12 days. cis-1,2-DCE was the major intermediate formed from day 3 to 14 and reached its transient peak at 1.5 μM on day 9. No trans-1,2-DCE or 1,1-DCE was observed in this effluent over the experimental period. As cis-1,2-DCE was reduced, VC transiently accumulated (peak of ~3 μM on day 14). However, VC was fully reduced to ethene by 21 days. By 23 days, every chlorinated ethene (TCE, DCE, and VC) was reduced to below the analytical detection limit, and effluent ethene was almost stoichiometric with influent TCE by day 30.

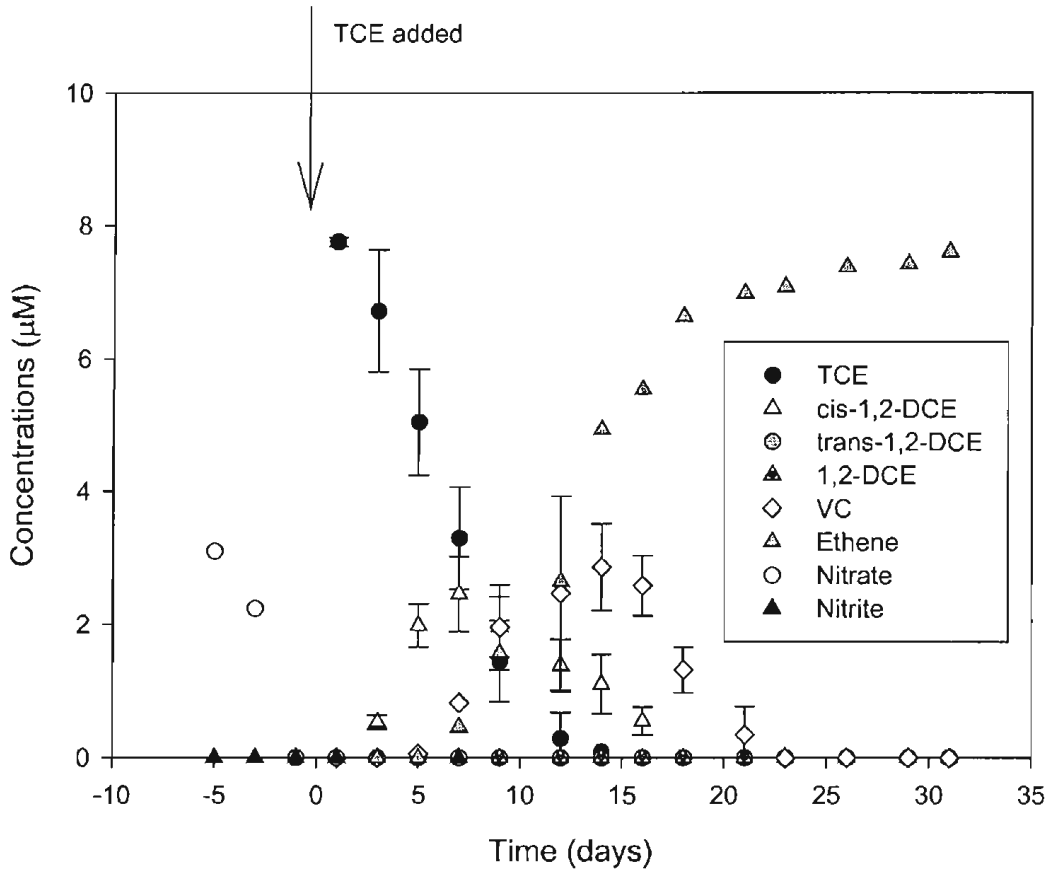

Figure 3.13 TCE, DCE, VC, and ethene concentrations in the effluent from the TCE-dechlorinating MBfR (Left Y-axis: all compounds (μM))

As shown in Figure 3.14, the rate of TCA biotransformation was somewhat slower than for the other two chlorinated solvents (see Figure 3.12 and Figure 3.13), but TCA was fully reduced by 24 days. DCA reached at its highest concentration (~ 1 μM) at day 8, but then disappeared. CA gradually increased to 6.8 μM and reached its steady-state condition (c. 5.5 μM) around day 17. Ethane was not detected, which suggests that reduction stopped at CA. However, the steady-state concentration of CA was less than the amount of TCA removed, which may mean that CA was degraded by hydrolysis to ethanol, which could not be detected, or that the ethane at the μM level was not detected.

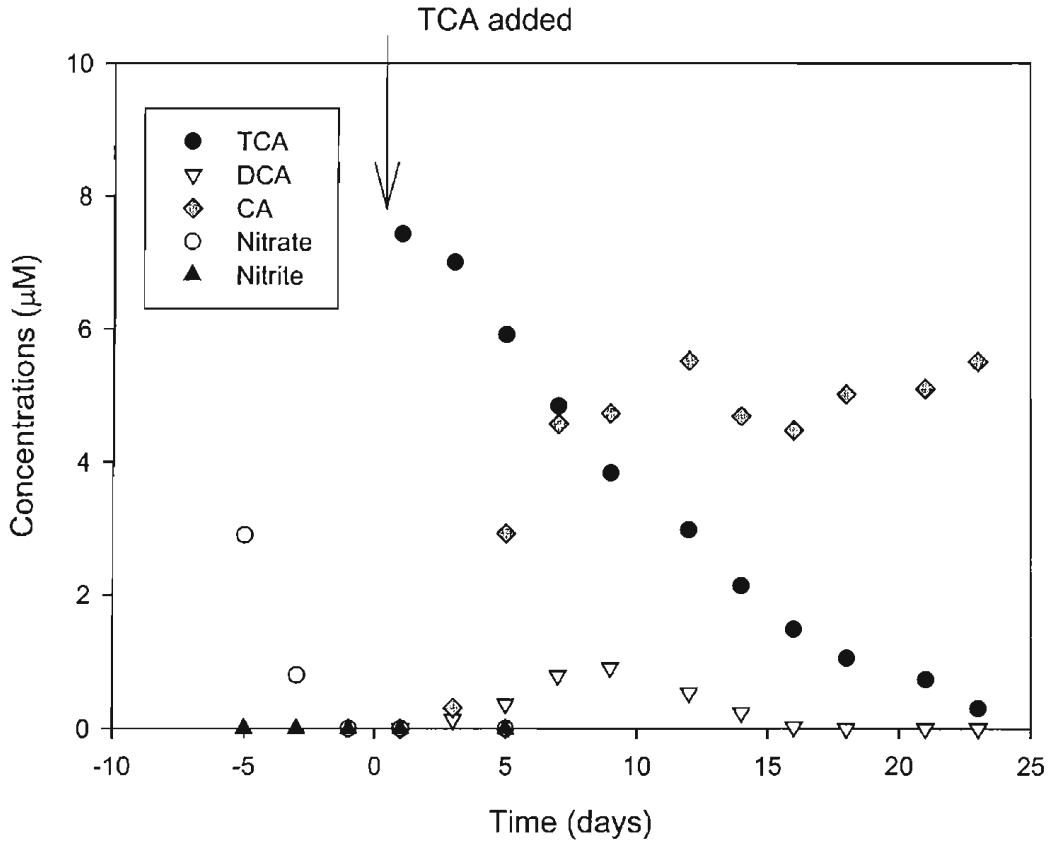

Figure 3.14 TCA, DCA, and CA concentrations in the effluent from the TCA-dechlorinating MBfR (Left Y-axis: all compounds (μM))

Influence of Sulfate

As shown in Figure 3.15, from day 23, the effect of sulfate reduction on CF removal was investigated by increasing the sulfate content in the nitrate medium in five steps from 50 μM to 1,000 μM. The sulfide concentration increased as sulfate concentrations added increased. Up to a concentration of 100 μM, sulfate had no significant effect on the transformation of CF. At higher concentrations, however, DCM and CM transformations were less complete. This result implies that competition for hydrogen interfered with the full reductive dechlorination of CF.

On day 53, the H_2 pressure was increased to 4.0 psi. The CF, DCM, and CM concentrations in the effluent gradually decreased and reached steady state on day 75. From day 75, the H_2 pressure was reduced to 2.5 psi, and the sulfate concentration in the influent was changed in order to investigate whether the MBfR responds rapidly to sulfate and is consistent with competition for H_2. From day 83 to the end, CF, DCM, and CM concentrations depended upon the sulfate concentration in a manner consistent with competition for hydrogen: a rapid increase in concentration with more sulfate, and vice versa. This confirms that the dechlorination of CF is controlled by the availability of hydrogen, and increased sulfate decreases availability for reductive dechlorination.

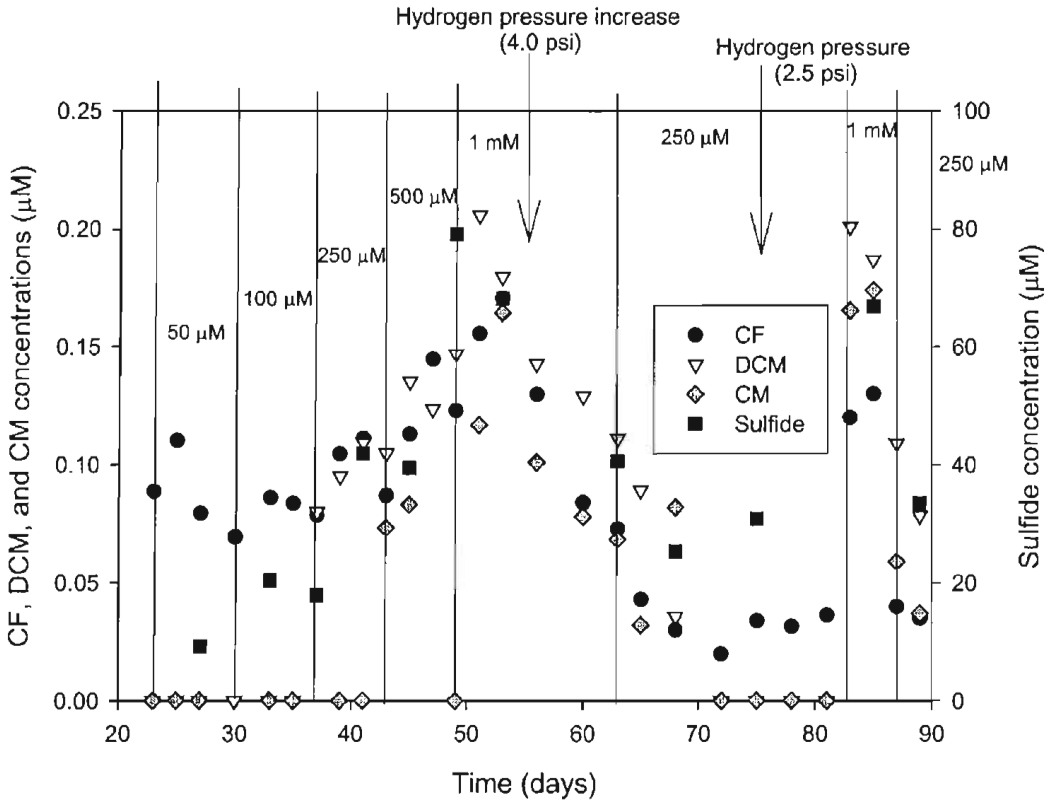

Figure 3.15 Dechlorination of CF with different sulfate concentration and H2 pressure. Left Y-axis: CF, DCM, CM concentration (µM); Right Y-axis: sulfide concentration (µM))

Figure 3.16 shows the influence of sulfate concentration and hydrogen pressure upon the dechlorination of TCE. As soon as sulfate was added, TCE and VC appeared, while the amount of ethene decreased. At higher concentrations of sulfate, cis-1,2-DCE also appeared. Increasing the H_2 pressure to 4 psi on day 53 reversed the trends. These results indicate competition for H_2 as the common electron donor. Whereas cis-1,2-DCE and VC gradually decreased, the ethene concentration in the effluent was nearly equi-molar with the TCE removed. From day 83 to the end, TCE, DCE, VC, and ethene concentrations changed immediately with sulfate levels in a manner similar to the CF case, which again confirms that reductive dechlorination of TCE competed with sulfate reduction for available H_2.

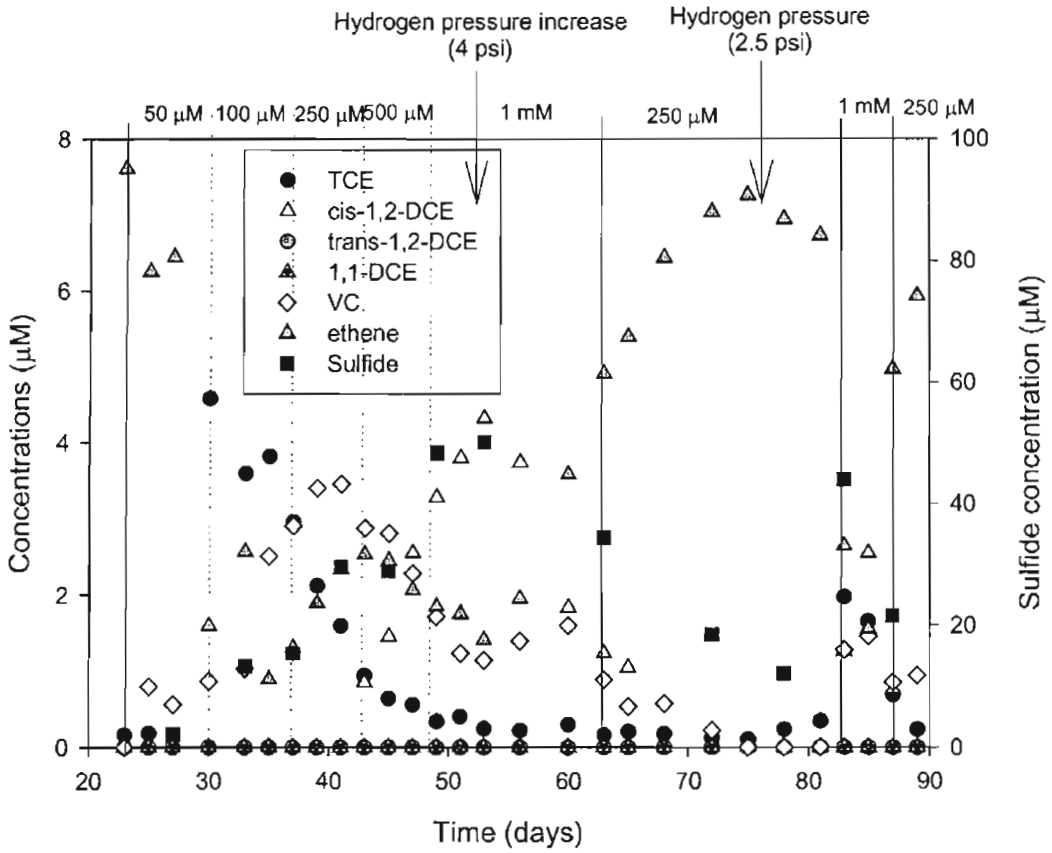

Figure 3.16 Dechlorination of TCE under different sulfate concentration and H_2 pressure. (Left Y-axis: TCE species (μM); Right Y-axis: sulfide concentration (μM))

Figure 3.17 shows the influence of sulfate and H_2 pressure upon the dechlorination of TCA. 50 μM and 100 μM sulfate initially caused the TCA concentration to increase, but it gradually declined after that. However, DCA became a major transformation product, while CA declined for 250 to 1,000 mM sulfate, indicating that the reduction of TCA became less complete with more competition from sulfate reduction. On day 53, the H_2 pressure was increased to 4.0 psi. DCA gradually decreased, and CA increased, which again illustrate the competition for H_2. After day 75, the H_2 pressure was restored to 2.5 psi, and the sulfate concentration in the influent was increased in order to investigate whether TCA response is rapid and consistent with competition for H_2. From day 83 to the end, TCA and intermediates rapidly changed with sulfate concentration in manners consistent with competition between sulfate reduction and dechlorination using H_2.

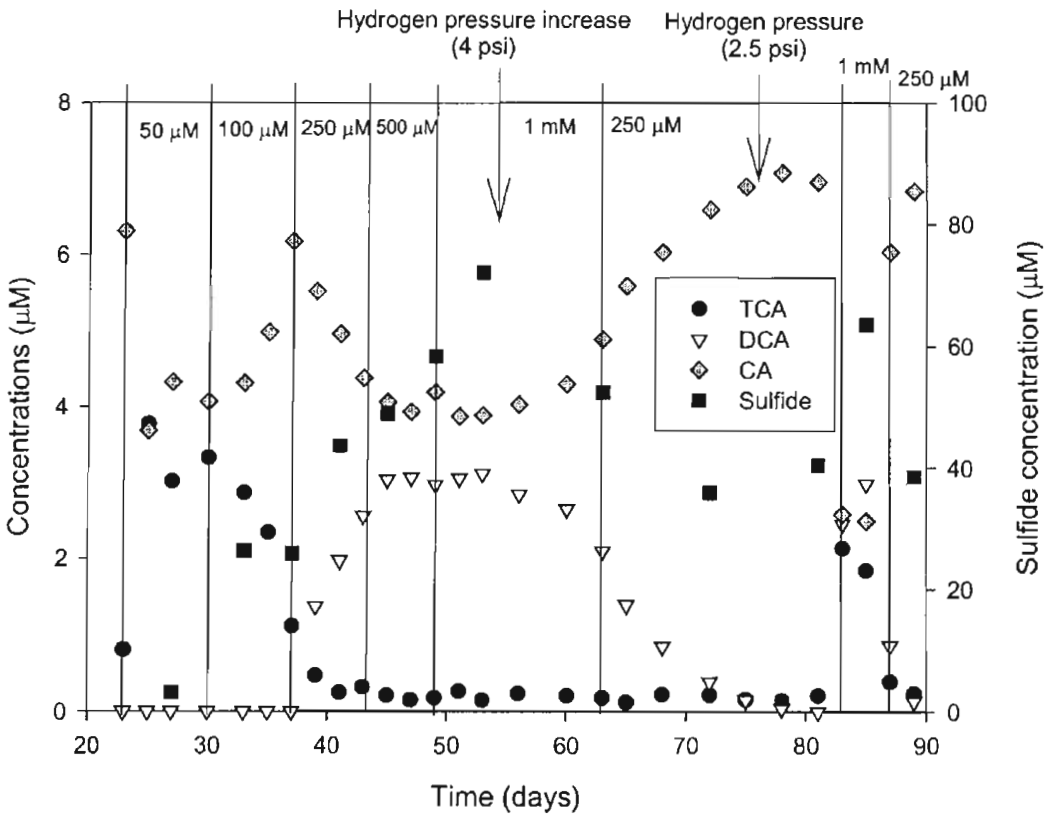

Figure 3.17 Dechlorination of TCA under different sulfate concentration and hydrogen pressure. (Left Y-axis: TCA species (μM); Right Y-axis: sulfide concentration (μM))

Dechlorination of Mixed Chlorinated Solvents

The objective of this phase of this work was to observe whether three kinds of chlorinated compounds could be dechlorinated simultaneously in MBfRs using hydrogen as electron donor. Figure 3.18 shows the concentrations of chloroform, TCE, and TCA in the effluent. Intermediates of each compound appeared in the experimental period, but are not displayed in Figure 3.18 to avoid conjestion. The MBfRs' operation was initiated with the influent containing 8.4 μM (1 mg/L) CF, 7.6 μM (1 mg/L) TCE and 7.5 μM (1 mg/L) TCA. All compounds were reduced to each form intermediate within three days of the addition. However, the removal rates for each compound were significantly different from each other. CF was reduced most quickly, with TCA and TCE lagging.

On day 33 (at a CF concentration near 0.8 μM), the reductions of TCE and TCA began to accelerate. These results suggested that reductive dechlorination of TCE and TCA may have been inhibited by CF. From day 51, the influent concentration of all chlorinated compounds was changed (from 1,000 to 2,500 μg/L) to evaluate the possible inhibitory effect of CF, as well as the reductive-dechlorination capacity of the acclimated MBfR. The rate of biotransformation for all compounds increased so that all input VOCs were reduced to very low effluent concentration, regardless of the higher influent loading.

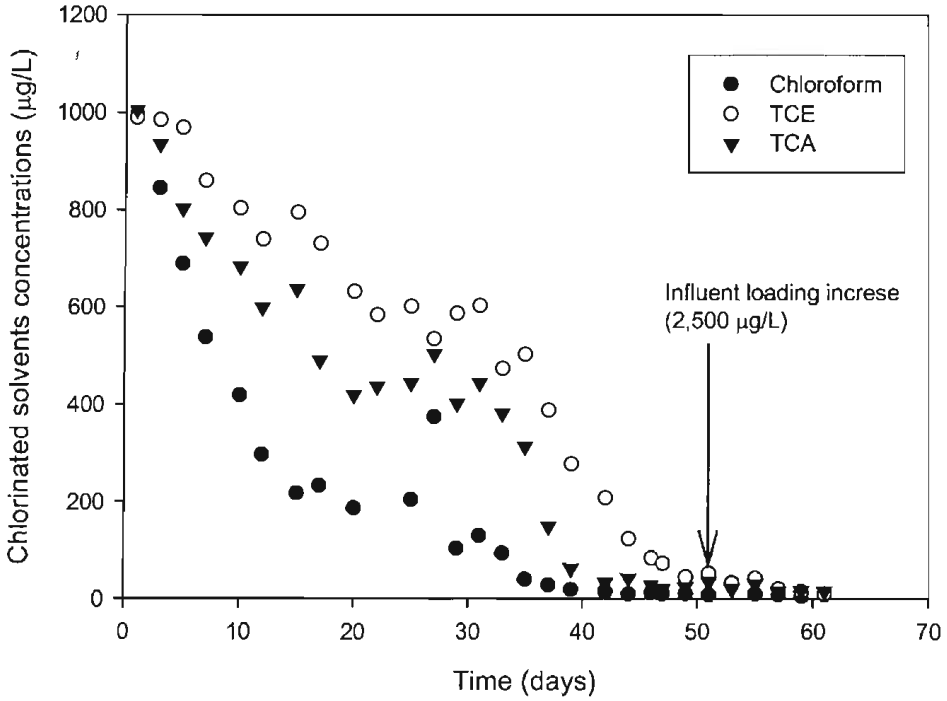

Figure 3.18 CF, TCE and TCA concentrations in the effluent from the MBfR fed with 5 mg/L of NO_3^--N and 1,000 µg/L of mixed chlorinated solvents. (Left Y-axis: all compounds concentration (µM))

Figure 3.19 combines the concentrations of the three input compounds with the intermediates in the effluent from MBfR. When 8.4 µM of chloroform (CF) was added, dichloromethane (DCM) transiently accumulated (as high as approximately 1.6 µM), and low levels of CM (chloromethane) (0.38 µM maximum) also were detected (Figure 3.19a). During this period of CF degradation, essentially no methane was produced (data not shown). Also, as the CF loading increased (after day 51), DCM and CM increased slightly.

As shown in Figure 3.19b, TCE was dechlorinated to vinyl chloride (VC) and ethene via a transient peak of cis-1,2-DCE (disappeared after day 31). Probably cis-1,2-DCE was produced and transformed to VC rapidly from day 31. No trans-1,2-DCE and 1,1-DCE were observed in this effluent over the experimental period. In this study with mixed VOCs, the dominant reduction product was VC, not ethene, which was dominant with TCE alone. It is possible that CF inhibited reduction of TCE or its intermediates. Bagley et al. (2000) observed complete inhibition of perchloroethene (PCE) dechlorination at 4 µM of CF, and Maymo-Gatell et al. (2001) found that 1.6 µM CF completely inhibited cis-DCE dechlorination. Also, recently Duhamel et al. (2002) reported the CF most strongly inhibited by the final conversion of VC to ethene, with complete inhibition occurring at an aqueous CF concentration of 2.5 µM. The incomplete reduction of VC to ethene is consistent with the findings Duhamel et al. (2002). However, significant reduction to ethene occurred.

1,1,1-trichloroethane (TCA) was removed in the MBfR without lag (See Figure 3.19c), and modest amounts of 1,1-dichloroethane (DCA) were formed initially. Chloroethane (CA) started to accumulate in the effluent from day 38. The sum of CA and DCA did not equal the removal of TCA, and this suggests that ethane or ethanol was formed as a final dechlorination product. Based on results from Chen et al. (1999), accumulated CA can be partially converted to ethane. However, ethane was not found. It seems like that TCA dechlorination was partially inhibited by CF, because TCA removed quickly when CF concentration decreased to 0.4 μM.

In summary, the most important finding is that all three VOCs were reductively dechlorinated simultaneously in the MBfR. The time to reach full reduction was longer with the three VOCs together (compare Figure 3.18 with Figure 3.12– Figure 3.14). This may have been caused by inhibitory interactions among the VOCs, but it also may have been more the result of competition for H_2 or different inoculum sizes. The acceleration in the reductions of TCA and TCE around day 30 suggests that CF may have inhibited reductive dechlorination, but it also may have been due to changes in biomass. Despite possible interactions among the VOCs, the microbial community in the MBfR rapidly acclimated to all three and brought about simultaneous reductions.

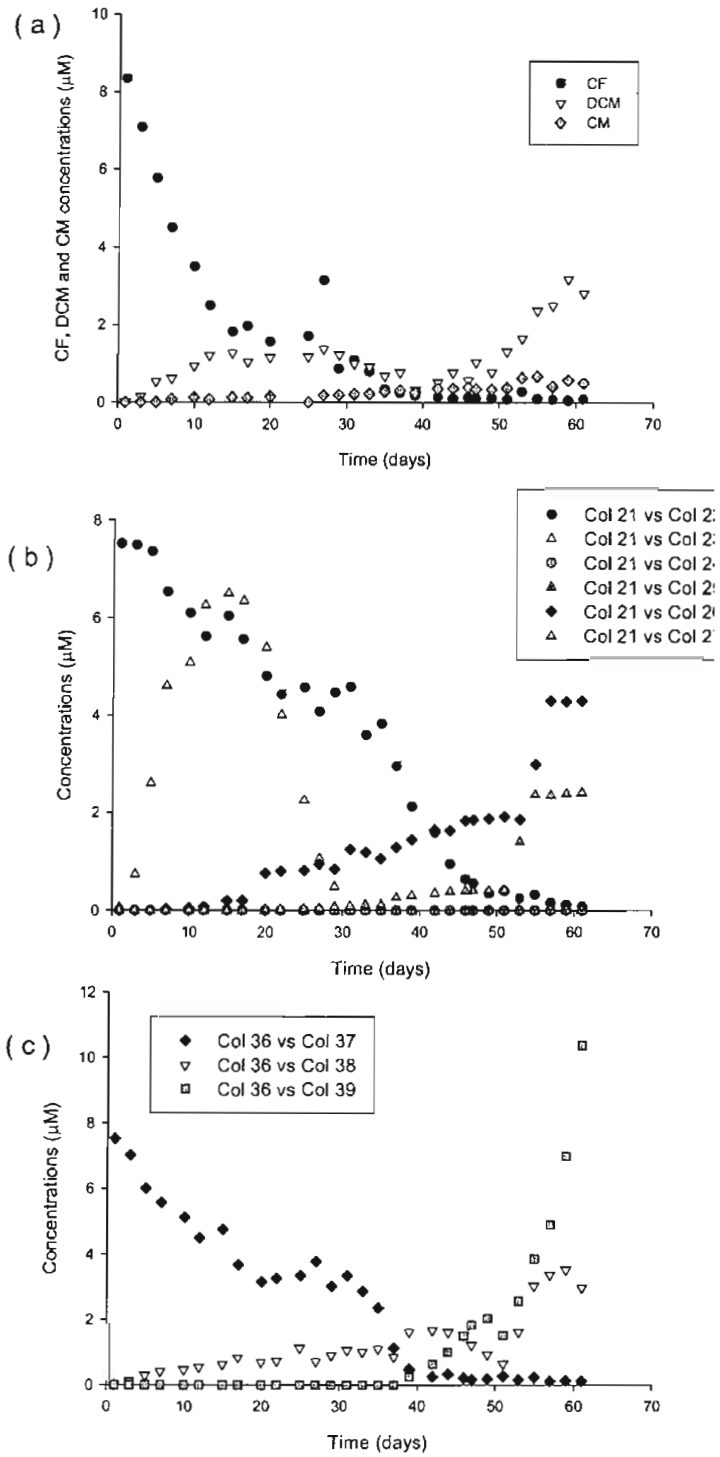

Figure 3.19 Chlorinated solvents and intermediates concentrations in the effluent from the MBfR

CHAPTER 4

HYDRAULIC MODELING

BACKGROUND

Previous research with the pilot-scale MBfR has shown that the reactor hydraulics has the largest impact on the overall performance of the process (Adham et al., 2004). The flow condition within the reactor determines if the nutrients and contaminants will be evenly dispersed throughout the reactor, thereby enabling the entire membrane surface to be utilized. Modifications to the physical configuration of the reactor can have dramatic impacts on process performance.

The objective of the hydraulic modeling was to develop a hydrodynamic model of the existing MBfR to aid in identifying how the hydraulics of the reactor could potentially be used to improve the performance of MBfR system.

APPROACH

Hydraulic modeling was achieved using computational fluid dynamics (CFD), a computer-based methodology for the solution of the fundamental equations of fluid flow. The equations that govern a process of interest, usually in partial differential form, are solved numerically to obtain the properties of flow, such as velocity, pressure and turbulence.

The CFD model used in this project is a commercial software package, Fluent 6.1 (Fluent Inc., NH, USA). The preprocessing program is Gambit 2.1 (Fluent Inc., NH, USA). The first step of the CFD modeling was using Gambit to create a reactor based on the geometry of the MBfR system and specify the fluid and solid zones in the reactor. The fluid zones were divided into fine elements where the mass conservation equations and momentum conservation equations had to be solved. Inlet and outlet boundary conditions (e.g., inlet velocity) were given to the model. Initial solution values were setup to start the program and iterations of solutions continued until the solutions converged to a set of criteria. Post processing was utilized to plot velocity contour graphs and generate particle tracking to build residence time distribution curves.

The CFD model was validated with tracer studies of the existing bench-scale system. An inert chemical compound was injected to the system, and the concentration of the compound was recorded to generate the residence time distribution. The performance of the bench-scale reactors under different flow conditions was modeled and compared with the results of tracer tests performed on the bench-scale reactor.

Due to the size of the pilot-scale reactor, instead of modeling individual membrane fibers as done for bench-scale reactor, the pilot-scale reactor was modeled using porous media approach.

BENCH-SCALE RESULTS

The CFD model was created based on the dimensions of the bench-scale MBfR described in Table 2.1. Figure 4.1 illustrates the MBfR reactor setup in the CFD model. The CFD model simulated the flow through mode, thus only the main tube with 32 membrane fibers was modeled.

The model simulated flow rates at 100 and 150 mL/min. Figure 4.2 and Figure 4.3 show the profiles of velocity-magnitude contour plots in the bench-scale MBfR reactor at a flow rate of 150 mL/min. As illustrated in the color bar, the red color represents the highest velocity and the blue color represents the lowest velocity. Figure 4.2 is a plan view of the velocity contour plot showing that there are small areas of dead zones with very low velocity (dark-blue zones) in the inlet and outlet areas. However, the flow is nearly uniform inside the reactor for the entire length of the fibers. Figure 4.3 gives a close look of the velocity profile radially across the reactor. The fibers partially block flow and slightly slow down the flow velocity adjacent to them.

Tracer Results

After the steady-state velocity field was generated, a Lagrangian trajectory approach was used to predict the trajectories of inert tracer particles. Figure 4.4 shows the path lines of particles colored by residence time in the reactor. The residence time increases as the color changes from blue to red. Based on a sensitivity analysis of the number of the particles virtually injected in the reactor, around 1300 particles were used for the CFD modeling so that a histogram of the particle residence time could be generated to create a representative distribution. The variation in color of particles at the system outlet indicates that some particles exit the system faster than others do. A pulse input applying to an ideal reactor with uniform velocity through the whole reactor would generate the same pulse output, a delta function. However, in reality, the output is more likely a distribution; the tighter the residence time distribution, the better reactor hydraulics is. Based on the velocity profile at the cross section area in Figure 4.3, the water can go through the reactor faster between the circles and slower between adjacent fibers. It is important to note, however, that the fibers are not uniformly distributed in the reactor as assumed in the hydraulic model.

In order to validate the hydrodynamic model, tracer tests were performed on the bench-scale MBfR in a flow through mode using main tube without biofilm. Figure 4.5 and Figure 4.6 show the examples of residence time distribution calculated from the results of CFD simulation, along with results of a bench-scale tracer test at the same flow rate, 150 and 100 mL/min respectively.

Table 4.1 and Table 4.2 are comparisons of the mean residence time and normalized variance of the residence time distribution from the CFD model and the bench-scale tracer tests. At a flow rate of 100 mL/min, the mean residence time of the CFD model and tracer test were 7.94 and 8.29 seconds, respectively. At flow rate of 150 mL/min, the mean residence time of the CFD model and the tracer test were 5.67 and 7.22 seconds, respectively. The shape of the distributions are very similar between the results of the CFD modeling and the bench-scale tracer tests, although the difference of the mean residence time and normalized variance are in the range of 5 to 27 percent. These differences might be partially caused by the difficulties of taking samples at very short residence time of bench-scale study.

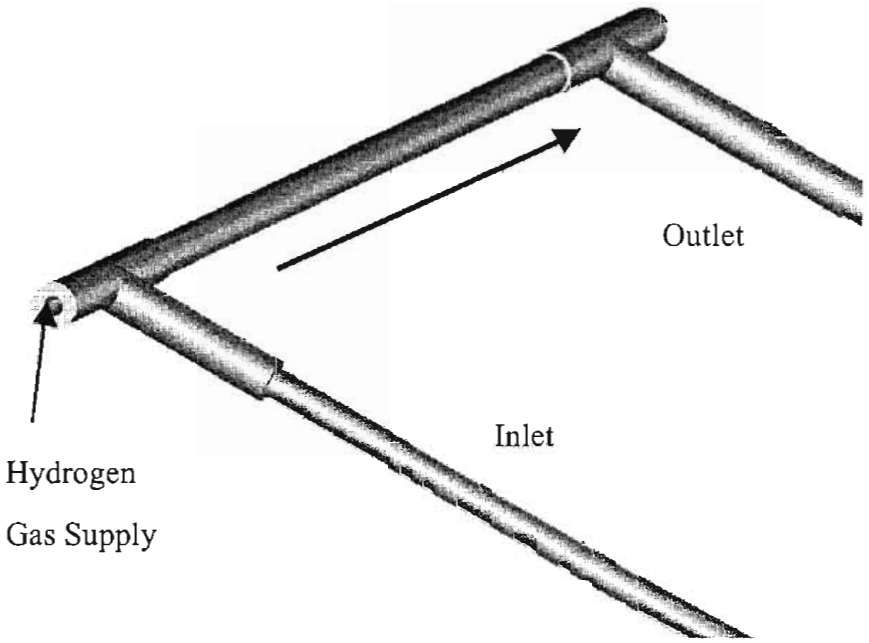

Figure 4.1 CFD model of the bench-scale MBfR reactor

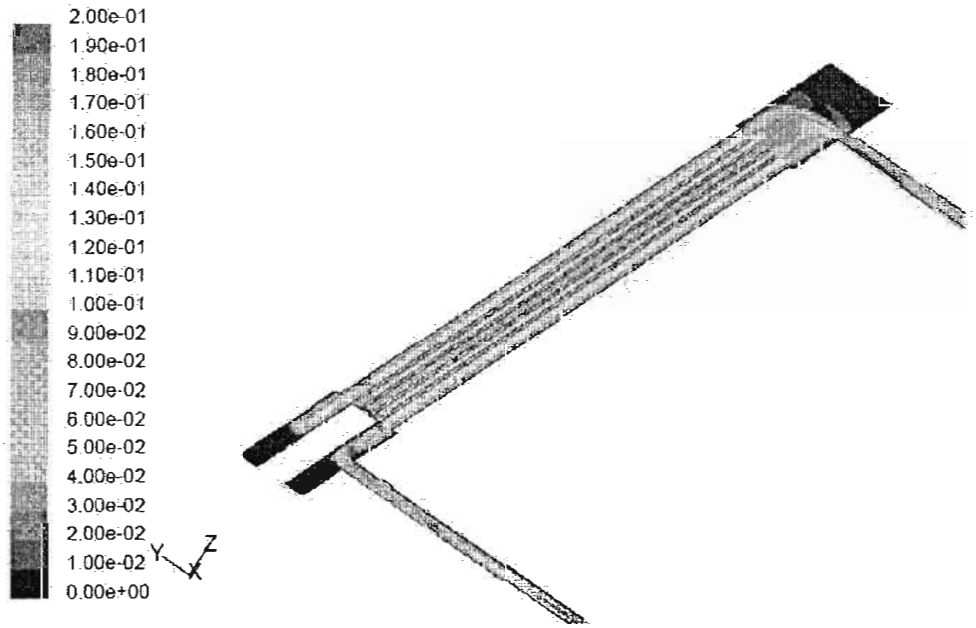

Figure 4.2 Plan view of velocity profiles in the bench-scale MBfR reactor, color bar is in the unit of m/sec

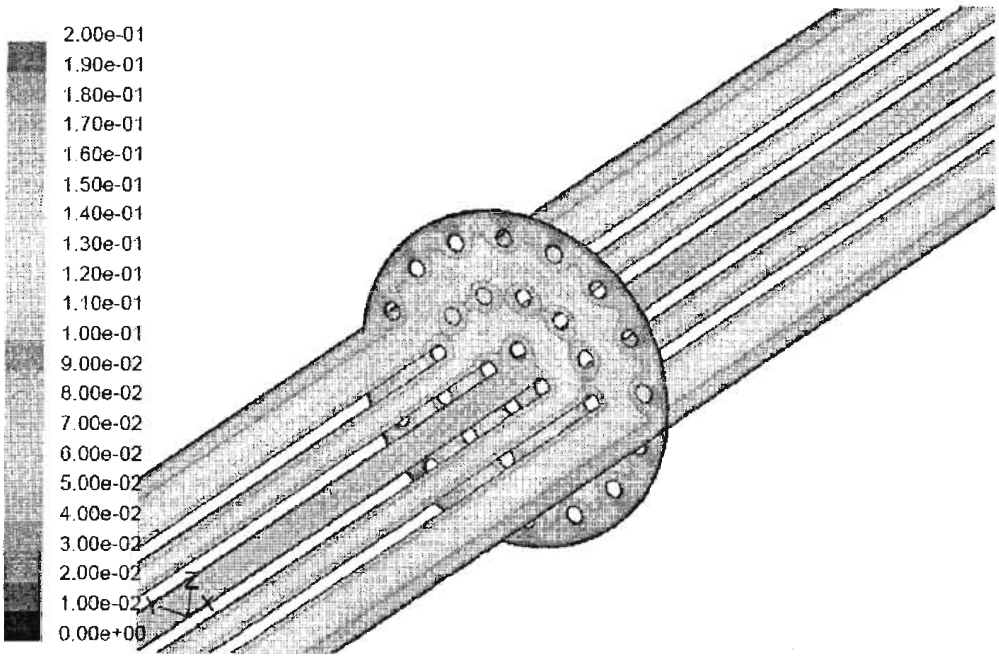

Figure 4.3 Velocity profiles of the bench-scale MBfR reactor, color bar is in the unit of m/sec

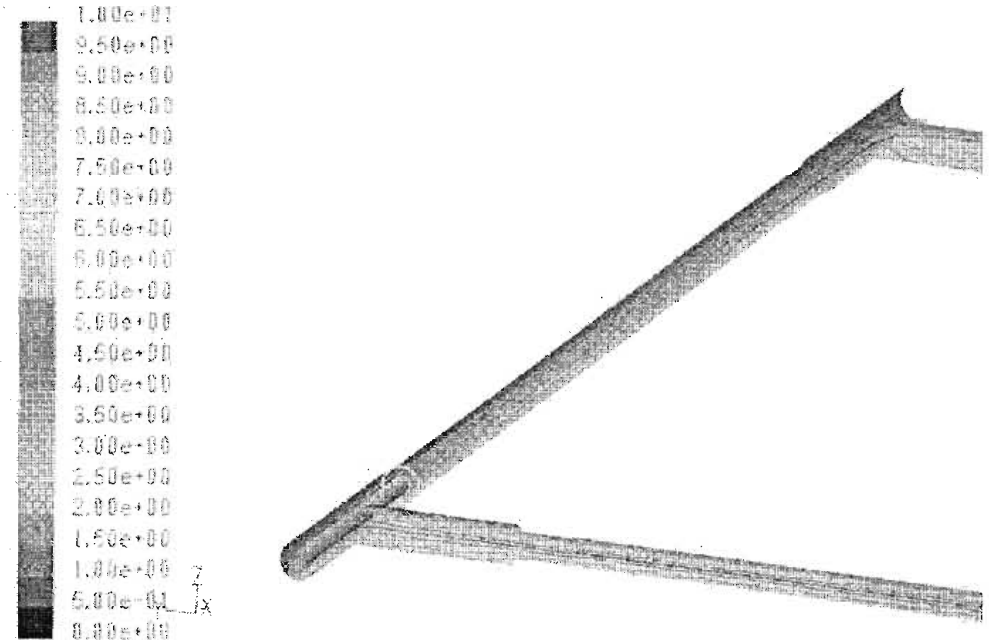

Figure 4.4 Particle trajectories in the bench-scale MBfR, color bar represents the residence time in seconds

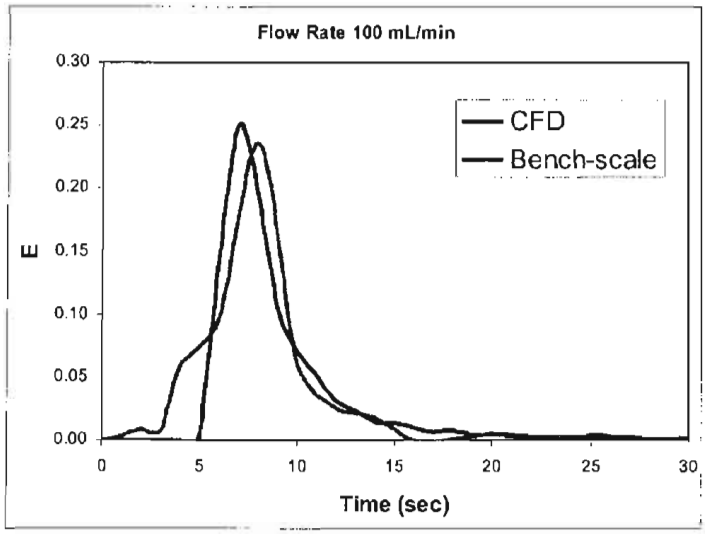

Figure 4.5 Residence-time distributions of a 100-mL/min tracer test and corresponding CFD model

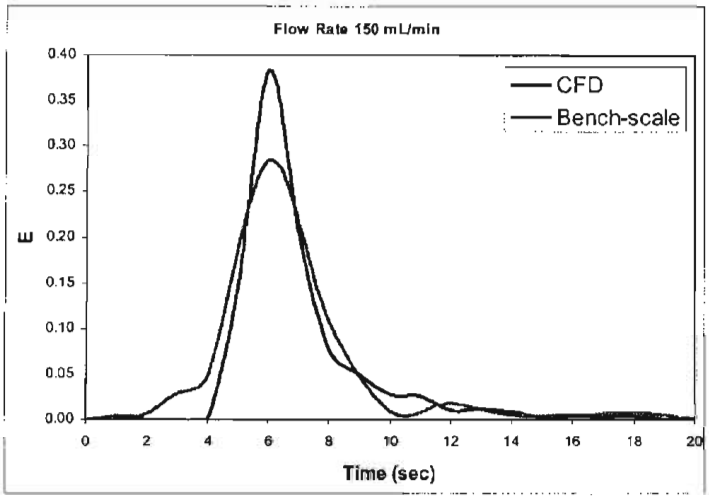

Figure 4.6 Residence-time distributions of a 150-mL/min tracer test and corresponding CFD model

Table 4.1 Comparison of mean residence time

Q (mL/min)	CFD (sec)	Bench-scale (sec)	Difference
100	7.94	8.29	5%
150	5.67	7.22	27%

Table 4.2 Comparison of normalized variance of residence time distribution

Q (mL/min)	CFD	Bench-scale	Difference
100	0.25	0.207	21%
150	0.348	0.283	23%

Surface Roughness

The bench-scale tracer tests were originally performed on a new MBfR reactor without biofilm. Additional tracer tests were performed with biofilm to investigate the impact of biofilm on the hydraulic conditions. Table 4.3 shows the results for mean residence time of the MBfR with and without biofilm. The differences between the mean residence time with and without are insignificant, indicating that the biofilm did not have impact on the hydraulic condition.

Table 4.3 Mean residence time of tracer tests at MBfR reactor with and without biofilm

Q (mL/min)	Without Biofilm (sec)	With Biofilm (sec)	Difference
100	8.29	8.11	2%
150	7.22	7.41	3%

A similar analysis was conducted using CFD modeling. The bench-scale CFD model with wall roughness of 100 μm (representing the average thickness of biofilm measure) was modeled to simulate a biofilm on the membrane surface. The model was performed at flow rate of 150 mL/min. The difference of the mean residence time between with and without biofilm (wall roughness) was approximately 10%, which confirmed the conclusion of bench-scale tracer tests that biofilm has no significant impact on hydraulic condition.

Impact of Velocity and Shear Stress

The shear stress is defined as a tangential force divided by the area (force/area) on which it is applied. The shear stress expressed the tendency of a fluid to be "pulled apart" (sheared) by a differential force. Mathematically, the shear stress is defined as the viscosity of the fluid multiplying the velocity gradient perpendicular to the fluid flow.

As observed in previous pilot testing (Adham et al., 2004), a non-uniform flow condition in the reactor can create dead zones and/or zones of high velocity, which cause non-uniform shear forces on the membrane surface creating a wide distribution of biofilm thicknesses in the reactor. The velocity and shear forces on the biofilm can control the thickness and density of the biofilm, as well as what organisms may be able to withstand the environment.

To better understand the important relationship between the shear stress and velocity, the shear force in the bench-scale reactor was simulated using CFD at different flow rates. Table 4.4 shows the average shear stress on membrane fibers at two flow rates. The average shear stress on the membrane fibers is higher when the average flow rate is higher. The shear stress is lowest on fibers close to the reactor wall where the velocity is lower, and highest between the wall and the center of the reactor, where the velocity is highest (see Figure 4.3).

Table 4.4 Average shear stress on membrane surface at different flow rates

Flow rate	Average shear stress on fibers close to center (pascal)	Average shear stress on fibers midway between the wall and the center (pascal)	Average shear stress on fibers close to reactor wall (pascal)	Average shear stress (pascal)
150 mL/min	0.94	1.03	0.82	0.92
100 mL/min	0.63	0.69	0.55	0.61

The modeling results demonstrated that an increased velocity resulted in higher shear stress. As a result, a thinner biofilm would be expected. At the conclusion of the bench-scale study, the biofilm thickness of the bench-scale MBfR was measured using confocal laser scanning microscopy. At recirculation rate of 150 mL/min and average bulk flow velocity of 570 cm/min, the biofilm thickness was in the range of 70-95 μm. In previous research with the bench-scale MBfR (Lee and Rittmann, 2002), the biofilm thickness was in the range of 110-180 μm at a bulk fluid flow velocity of approximately 100 cm/min. The biofilm thickness results show that the current bench-scale MBfR with a higher velocity (150 mL/min) resulted to a denser and thinner biofilm. This, in turn, agreed with the modeling results (higher velocity resulted in higher shear stress) corresponding to the presence of a thinner biofilm.

PILOT-SCALE RESULTS

The bench-scale modeling results and biofilm thickness measurements indicated that velocity has a strong impact on the biofilm thickness. The non-uniform biofilm thickness observed in the pilot-scale MBfR was caused by the fact that the pilot-scale unit has a non-uniform flow condition. It was not feasible to operate the pilot unit with high recirculation rate as the bench-scale reactor; therefore, the mixing introduced by the high recirculation rate at the bench-scale reactor was not possible in the pilot-scale system.

The objective of the pilot-scale hydraulic modeling was to identify critical hydraulic conditions that existed in the pilot reactor. A porous media model was used for simulating pilot-scale reactor, based on the total flow resistance in the porous region. This model incorporated a momentum source term to the standard fluid flow equations. The source term was composed of a viscous loss term and an inertial loss term. This momentum sink contributes to the pressure gradient in the porous cells, creating a pressure drop that is proportional to the fluid velocity. Both the viscous resistance coefficient and inertial resistance coefficient were determined by empirical results. The differential pressures were measured in the pilot unit at different locations and at different flow rates, then the viscous resistance and inertial resistance coefficients were obtained from the regression of the data between pressure decay and velocity.

The porous media model was simulated first without the porous media zones, and the velocity field without porous media parameters was obtained after the model converged. Then, the

viscous resistance and inertial resistance coefficients, as well as the porosity, were assigned to the porous media zones to simulate the porous media model.

Tracer Results

Similar to the bench-scale modeling, the calculation of pilot-scale model with porous media zones was iterated until the solutions reached the steady-state. A Lagrangian trajectory approach was used to generate the residence time distribution in the reactor. Based on the velocity profile shown in Figure 4.7, the flow is non-uniform in the pilot-scale MBfR. Inlet and outlet areas with red color indicate high velocities regions.

Tracer tests were also conducted on the pilot-scale MBfR at flow rates of 4, 5, and 6 gpm. Table 4.5 and Table 4.6 are comparisons of the mean residence time and normalized variance of the residence time distribution from the CFD model and the pilot-scale tracer tests. The difference of the mean residence time and variance are in the range of 36 to 96 percent showing that the CFD model did not correctly simulate the pilot-scale MBfR. It is interesting to note that the mean residence times calculated from CFD model were similar to the theoretical detention time (reactor volume divided by average flow rate), as shown in Table 4.5. However, the pilot-scale mean residence times were shorter than the theoretical detention time, indicating that short-circuiting existed in the system. The condition is typically considered short-circuiting when some fluid elements exit the reactor earlier than the theoretical detention time. Although the CFD results did not match the pilot-scale trace tests, the trend of having smaller a variance at a higher flow rate is the same for both CFD modeling and pilot-scale tracer tests. The smaller the variance, the tighter the residence time distribution, which is a more desired uniform flow condition.

One possible reason that the CFD model did not simulate the short-circuiting of the pilot-scale MBfR was that the membrane fibers were not uniformly distributed inside the pilot-scale MBfR. For this simulation, the porous media model assumed the same resistance coefficients and porosity for the entire reactor. The model does have the capability to assign zones with individual resistance coefficients and porosities. However, detailed pilot-scale data would be required to accurately define these model inputs. Additionally, numerous turbulent models and wall functions are available in the CFD program, which would also require extensive pilot-scale data to properly calibrate the model. Once the model is properly calibrated, it can be effectively used to optimize the pilot- and full-scale reactor.

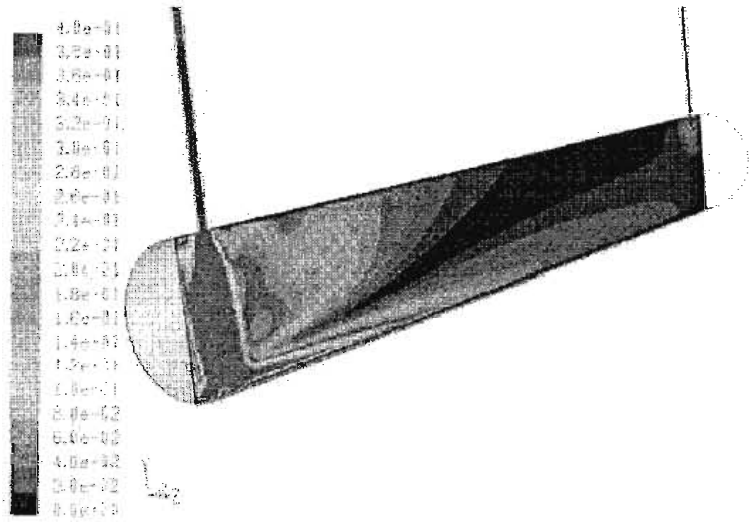

Figure 4.7 Velocity profiles of the pilot-scale MBfR reactor at 6 gpm, color bar is in the unit of m/sec

Table 4.5 Comparison of mean residence time

Q (gpm)	CFD (sec)	Pilot-Scale Testing (sec)	Difference	Theoretical Detention Time (sec)
4	70	42	68%	68
5	59	30	96%	54
6	49	28	76%	45

Table 4.6 Comparison of normalized variance of residence time distribution

Q (gpm)	CFD	Pilot-Scale Testing	Difference
4	0.299	0.826	64%
5	0.293	0.561	48%
6	0.286	0.450	36%

CHAPTER 5

REGULATORY APPROVAL

Previously, the project team had successfully performed extensive bench- and pilot-scale testing of the MBfR to treat groundwater contaminated with nitrate and perchlorate for potable water production. However, there was limited interaction with state regulators during the initial development of the MBfR. As a result, the project team planned to conduct two workshops with state regulators to allow input to be provided at both the beginning and end of this research. The goal of these workshops were to document and identify the specific requirements that would need to be satisfactorily addressed for obtaining future California Department of Health Services (CaDHS) approval of MBfR process for the production of potable water.

FIRST PROJECT WORKSHOP

The first workshop between the project team and the CaDHS Water Treatment Committee (WTC) was held on September 23, 2003 (via conference call) to discuss the project scope of work and address any comments from CaDHS on their understanding of the MBfR process. Included in Appendix A are a letter from Dr. Rick Sakaji regarding comments on the MBfR process from a previous meeting (March 17, 2003) and meeting minutes of the project workshop conducted on September 23, 2003. Feedback from the CaDHS WTC was constructive and positive with regards to the status of the MBfR process. Dr. Sakaji specifically identified that the MBfR research, to-date, has been focused on bench- and pilot-scale testing. Although the WTC was confident in the process and consider the MBfR to be a promising technology, their main recommendation regarding future approval of the MBfR was the need to demonstrate the process on a larger scale (i.e., large pilot- and/or full-scale system). Other recommendations included:

- The need to investigate post-filtration requirements for removing sloughed biomass;
- Demonstrating the need for disinfection; and
- Determining alternative applications beside perchlorate. The WTC suggested that nitrate treatment might be a more immediate application as opposed to perchlorate.

REVIEW OF DRAFT FINAL REPORT

According to the original project scope, a second regulatory workshop was planned to discuss the project findings. Instead, the CaDHS WTC requested to review the draft final report and provide additional input/comment, since this research was primarily focused on bench-scale studies. Based on the first regulatory workshop, the WTC was more interested in discussing results of a pilot-scale study. As a result, any further comments from the WTC regarding the current MBfR research will be included in the final report submittal for this project.

CHAPTER 6

SUMMARY AND CONCLUSIONS

Bench-Scale Experiments with a Range of Oxidized Contaminants

Bench-scale experiments with the H_2-based MBfR documented the potential of the H_2-oxidizing bacteria in an MBfR to reduce a wide range of oxidized inorganic and organic contaminants. Previous research has demonstrated MBfR reduction of nitrate and perchlorate, and the results reported here extend the range to selenate, chromate, chloroform, TCE, and TCA. Reductions occurred quickly in all cases and responded positively to increased H_2 pressure. The systems showed a high degree of versatility towards different oxidized contaminants.

The reduction of Cr(VI) to Cr(III) began within the first two days of Cr(VI) addition. When the hydrogen pressure was increased from 2.5 psi to 4.0 psi, the average reduction of Cr(VI) was increased from 45 to 57%, confirming that chromate reduction is controlled by H_2 availability. When the influent Cr(VI) loading decreased, the average reduction of Cr (VI) increased to 63%, showing the expected trend that Cr(VI) reduction can be made more complete with a lower Cr(VI) loading. Chromate may have inhibited the reduction of sulfate, since almost no sulfide was produced.

Se(VI) was reduced to Se(IV) within one day of Se (VI) addition. Initially, Se (VI) was reduced exclusively to Se (IV), which is completely soluble; then, Se(IV) was reduced to Se°, which is a solid and retained with the biomass in the MBfR. Similar to the Cr-MBfR, increasing the H_2 pressure from 2.5 to 4 psi increased the Se(VI) reduction from 59 to 83%, while decreasing the selenate loading gave 99% Se(VI) removal. Selenate did not inhibit sulfate reduction, at least not at the concentrations present in the experiments, but a high level of sulfate reduction slowed selenate reduction by competing for H_2.

A series of short-term tests documented that nitrate reduction was not affected by the influent chromate or selenate load; the percentage chromate or selenate removal decreased with increased influent load; increasing H_2 pressure increased the reductions of chromate and selenate; and the optimal pH for chromate and selenate reduction was around 7.0 and 7.5, respectively. Furthermore, the Cr-reducing MBfR was immediately able to reduce selenate, while the Se-reducing MBfR was immediately able to reduce chromate.

When CF was added to a denitrifying MBfR, dechlorination of CF started immediately. DCM was formed transiently as a result of CF reduction, but was transformed to CM and methane after the CF had completely disappeared (3 weeks). When TCE was applied to a denitrifying MBfR, the TCE concentration in the effluent decreased rapidly. cis-1,2-DCE was the major intermediate formed, but it was reduced fully to VC and then to ethene within 3 weeks. The TCA biotransformation rate was somewhat slower than for the other two chlorinated solvents, but it too was reductively dechlorinated within 3.5 weeks. DCA accumulated transiently, and CA gradually increased to become the major end product. The reduction of CA to ethane was not detected, but CA accumulated less than TCA removed.

All three VOCs (CF, TCE, and 1,1,1-TCA) were dechlorinated simultaneously in an MBfR within approximately one month, despite possible inhibitory interactions among the VOCs. At very high sulfate influent concentrations, partial-dechlorination intermediates accumulated because the competition for H_2 interfered with the full reductive dechlorination of CF, TCE, and TCA.

Computational Fluid Dynamics Modeling

CFD modeling was used to identify important hydrodynamic characteristics of the bench-scale MBfR used in this study and pilot-scale MBfR used in a previous study. CFD modeling of the bench-scale MBfR was able to reproduce experimentally determined mean residence-time and its variance. The presence of biofilm had little impact on the residence time in tracer experiments or according to CFD modeling. Trajectory analysis showed that the bench-scale MBfR has no dead zones within the main reactor, but the flow velocity is lowest along the outer wall. The shear stress on the membrane, which helps control the biofilm's density and thickness, varies in proportion to the velocity.

For the pilot-scale MBfR, both pilot-scale tracer and CFD modeling show the trend that the higher flow rate generated tighter residence time distribution. The CFD modeling did not accurately simulate the short-circuiting as the results of the tracer tests. More pilot tests are necessary to validate the model.

Additional observations:
- The MBfR needs a uniform flow distribution that minimized dead zones and wall effects.
- Higher flow velocity increases shear stress, which helps to create a dense, thin biofilm.
- A uniform distribution system is desired to avoid dead zones or a flow condition with high variance.

Regulatory Approval

A workshop with CaDHS and held at the outset of the project yielded these key issues that need to be addressed by this and other research on the MBfR:

- The need to investigate post-filtration requirements for removing sloughed biomass;
- Demonstrating the need for disinfection and addressing the Surface Water Treatment Rule (SWTR); and
- Determining alternative applications beside perchlorate. The WTC suggested that nitrate treatment might be a more immediate application as opposed to perchlorate.

REFERENCES

Adamson, D.T. and Parkin, G.F. (1999) Biotransformation of mixtures of chlorinated aliphatic hydrocarbons by an acetate-grown methanogenic enrichment culture. Wat. Res. 33: 1482-1494

Adham, S., Gillogly, T., Lehman, G., Rittmann, B., and Nerenberg, R. (2004) Membrane biofilm reactor process for nitrate and perchlorate removal. AwwaRF and AWWA. Denver, Colorado.

Alvarez-Cohen, L. and McCarty, P.L. (1991) Effect of toxicity, aeration, and reductant supply on trichloroethylene transformation by a mixed methanotrophic culture. 57: 228-235

Alvarez-Cohen, L., McCarty, P.L., Boulygina, E., Hanson, R.S., Brussean, G.A. and Tsien, H.C. (1992) Characterization of a methane-utilizing bacterium from a bacterial consortium that rapidly degrades trichloroethylene and chloroform. Appl. Environ. Microbiol. 58: 1886-1893

Anderson, R.A. and Kozlovsky, A.S. (1995) Chromium uptake, absorption, and excretion of subjects consuming self-selected diets. Am. J. Clin. Nutr. 41: 117-1183

Aviado, D.M., Zakahari, S., Simann, J.A. and Ulsamer, A.G. (1976) Methyl Chloroform and Trichloroethylene in the Environment. CRC Press. Cleveland.

Aziz, C.E., Georgiou, G. and Speitel, G.E. (1999) Cometabolism of chlorinated solvents and binary chlorinated solvent mixtures using M-trichosporium OB3b PP358. Biotech. Bioeng. 65: 100-107

Barnhart, J. (1997) Occurrences, uses and properties of chromium. Regulatory Toxicology and Pharmacology 26: s3-s7

Bopp, L.H. and Ehrlich, H.L. (1987) Chromate resistance and reduction in *Pseudomonas fluorescens* strain LB300. Arch. Microbiol. 150: 426-431

Bouwer, E.J. and McCarty, P.L. (1983) Transformation of 1- and 2-carbon halogenated aliphatic organic compounds under methanogenic conditions. Appl. Envrion. Microbiol. 45: 1286-1294

Bradley, P.M. (2000) Microbial degradation of chloroethenes in groundwater systems. Hydrology Journal 8: 104-111

Buscheck, T.E., O'Reilly, K.T. and Hickman, G. (1997) In Situ and On-site Bioremediation (3); Battelle Press: Columbus, OH, Vol. 3, p. 149-164

Cervantes, C., Ji, G.Y., Ramirez, J.L. and Silver, S. (1994) Resistance to arsenic compounds in microorganisms. FEMS Microbiol. Rev. 15: 355-367

Chang, H.L. and Alvarez-Cohen, L. (1995) Model for the cometabolic biodegradation of chlorinated organics. Biotech. Bioeng. 45: 440-449

Chang, H.T., Rittmann, B.E., Amar, D., Heim, R., Ehlinger, O. and Lesty, Y. (1991) Biofilm detachment mechanisms in a liquid-fluidized bed. Biotech. Bioeng. 38: 499-506

Chen, C., Ballapragada, S.S., Puhakka, J.A., Strand, S.E. and Ferguson, J.F. (1999) Anaerobic transformation of 1,1,1-trichloroethane by municipal digester sludge. Biodegradation 10" 297-305

Chen, J.M. and Hao, O.J. (1996) Environmental factors and modeling in microbial chromium (VI) reduction. Water Environ. Res. 68: 1156-1165

Chidthaisong, A. and Conrad, R. (2000) Specificity of chloroform, 2-bromoethanesulfonate and fluoroacetate to inhibit methanogenesis and other anaerobic processes in anoxic rice field soil. Soil. Biol. Biochem. 32: 977-988

Cline, J.D. (1969) Spectrophotometric determination of hydrogen sulfide in natural waters. Limnol. Oceanogr. 14: 454-458

Coleman, N.V., Mattes, T.E., Gossett, J.M. and Spain, J.C. (2002a) Biodegradation of cis-dichloroethene as the sole carbon source by a beta-proteobacterium. Appl. Environ. Microbiol. 68: 2726-2730

Coleman, N.V., Mattes, T.E., Gossett, J.M. and Spain, J.C. (2002b) Phylogenetic and kinetic diversity of aerobic vinyl chloride-assimilating bacteria from contaminated sites. Appl. Environ. Microbiol. 68: 6162-6171

Davis, J.A., Kent, D.B., Rea, B.A., Maest, A.S. and Garabedial, S.P. (1993) Influence of redox environment and aqueous speciation on metal transport in groundwater: Preliminary results of tracer injection studies. In: Metals in Groundwater. Allen, H.E., Perdue, E.M. and Brown, D.S. (ed) Lewis, Boca Raton, FL. 223-273

de Best, J.H., Jongema, H., Weijling, A., Doddema, H.J., Janssen, D.B. and Harder, W. (1997) Transformation of 1,1,1-trichloroethane in an anaerobic packed-bed reactor at various concentrations of 1,1,1-trichloroethane, acetate and sulfate. Appl. Microbiol. Biotechnol. 48: 417-423

DeLeo, P.C. and Ehrlich, H.L. (1994) Reduction of hexavalent chromium by *Pseudomonas fluorescens* LB300 in batch and continuous cultures. Appl. Microbiol. Biotechnol. 40: 756-759

DiStefano, T.D., Gossett, J.M. and Zinder, S.H. (1991) Reductive dehalorination of high concentrations of tetrachloroethene to ethane by an anaerobic enrichment culture in the absence of methanogenesis. Appl. Environ. Microbiol. 57: 2287-2292

Dolan, M.E. and McCarty, P.L. (1995) Small column microcosm for assessing methane-stimulated vinyl-chloride transformation in aquifer samples. Environ. Sci. Technol. 29: 1892-1897

Doran, J.W. (1982) Advances in microbial ecology. Vol. 6, Plenium publishing Corp., New York, 1-32

Dragun, J. (1988) Element fixation in soil. In: *The soil chemistry of hazardous materials*. Greenbelt, MD: Hazardous Materials Control Research Institute, 75-152

Duhamel, M., Wehr, S., Yu, L., Rizi, H., Seepersad, D., Dworatzek, D,, Cox, E.E. and Edward, E.A. (2002) Comparison of anaerobic dechlorinating enrichment cultures maintained on tetrachloethene, cis-dichlororthene and vinyl chloride. Wat. Res. 36: 4193-4202

Egli, C., Scholtz, R., Cook, A.M. and Leisinger, T. (1987) Anaerobic dechlorination of tetrachloromethane and 1,2-dichloroethane to degradable products by pure cultures of Desulfobacterium sp. and Methanobacterium sp. FEMS Microbiol. Lett. 43: 258-261

Egli, C., Stromeyer, S., Cook, A.M. and Leisinger, T. (1990) Transformation of tetra- and trichloromethane to CO2 by anaerobic bacteria is a nonenzymic process. FEMS Microbiol. Lett. 68: 207-212

Ellis, D.E., Lutz, E.J., Odom, J.M., Buchanan, R.J., Bartlett, C.L., Lee, M.D., Harkness, M.R. and Deweerd, K.A. (2000) Bioaugmentation for accelerated in situ anaerobic bioremediation. Environ. Sci. Technol. 34: 2254-2260

Ensign, S.A., Hyman, M.R. and Arp, D.J. (1992) Cometabolic degradation of chlorinated alkenes by alkene monooxygenase in a propylene-grown xanthobacter strain. Appl. Environ. Microbiol. 58: 3038-3046

Ergas, S.J. and Reuss, A.F. (2001) Hydrogenotrophic denitrification of drinking water using a hollow fibre membrane bioreactor. J Water Supply Res. T. 50: 161-171

Erasin, B.R., Turner, A.P.F. and Wheatley, A.D. (1994) A fixed-film bioassay for the detection of micropollutants toxic to anaerobic sludges. Anal. Chim. Acta. 298: 1-10

Fathepure, B.Z. and Tiedje, J.M. (1994) Reductive dechlorination of tetrachloroethylene by a chlorobenzoate-enriched biofilm reactor. Environ. Sci. Technol. 28: 746-752

Federal Register (1989) National primary and secondary drinking water regulations; proposed rule. Fed. Regist. 54: 22062-22160

Freedman, D.L. and Gossett. J.M. (1989) Biological reductive dechlorination of tetrachloroethylene and trichloroethylene to ethylene under methanogenic conditions. Appl. Environ. Microbiol. 55: 2144-2154

Freedman, D.L. and Herz, S,D, (1996) Use of ethylene and ethane as primary substrates for aerobic cometabolism of vinyl chloride. Water Environ. Res. 68: 320-328

Fujita, A., Ike, M., Nishimoto, S., Takahashi, K. and Kashiwa, M. (1997) Isolation and characterization if a novel selenate-reducing bacterium, *Bacillus* sp. SF-1. J. Fermentation Bioeng. 83: 517-522

Gälli, R. and McCarty, P.L. (1989) Biotransformation of 1,1,1-trichloroethane, trichloromethane and tetrachloromethane by a Clostridium sp. Appl. Environ. Microbiol. 55: 837-844

Giovannoni, S.J. (1991) The polymerase chain reaction. In: *Nucleic Acid Techniques in Bacteria Systematics*. M. Goodfellow (ed) John Wiley & Sons, Chichester, England, 177-203

Gopalan, R. and Veeramani, H. (1994) Studies on microbial chromate reduction by *pseudomonas* Sp. in aerobic continuous suspended growth cultures. Biotech. Bioeng. 43: 471-476

Gossett, J.M. (1985) Anaerobic degradation of C1 and C2 chlorinated hydrocarbons. ESL-TR-85-38. U.S. Air Force Engineering and Services Center, Tyndall Air Force, Base, Fla.

Gossett. J.M. and Zinder, S.H. (1996) Microbiological aspects relevant to natural attenuation of chlorinated ethenes. Symposium of the Natural Attenuation of Chlorinated Organics in Groundwater. Dallas, TX, USEPA

Gupta, M., Sharma, D., Suidan, M.T. and Sayles, G.D. (1996) Biotransformation rates of chloroform under anaerobic conditions – I. Methanogenesis. Wat. Sci. 30: 1377-1385

Häggblöm, M.M. and Bossert, I.D. (2003) Halogenated Organic Compounds – A Global Perspective, in Dehalogenation: microbial processes and environmental applications, Häggblöm, M.M. and Bossert, I.D. Editors, Kluwer Academic Publishers: Boston, pp. 3-29

Haygarth, P.M. (1994) Global importance and global cycling of selenium. In: Selenium in the Environment. Frankenberger, W.T. and Benson, S. (ed) Marcel Dekker Inc., New York, 1-27

Hopkins, G.D. and McCarty, P.L. (1995) Field-evaluation of in-situ aerobic cometabolism of trichloroethylene and 3 dichloroethylene isomers using phenol and toluene as the primary substrates. Environ. Sci. Technol. 29: 1628-1637

Hopkins, G.D., Munakata, J., Sempriniti, .L. and McCarty, P.L. (1993) Trichloroethylene concentration effects on pilot field-scale in-situ groundwater bioremediation by phenol-oxidizing microorganisms. Environ. Sci. Technol. 27: 2542-2547

Jahng, D. and Wood, T,K. (1994) Trichloroethylene and chloroform degradation by a recombinant pseudomonad expressing soluble methane monooxygenase from Methylosinus trichosporium OB3b. Appl. Environ. Microbiol. 60: 2473-2482

Kashiwa, M., Nishimoto, S., Takahashi, K., Ike, M. and Fujita, M. (2000) Factors affecting soluble selenium removal by a selenate-reducing bacterium *Bacillus*. sp. SF-1. J. Biosci. Bioeng. 89: 528-533

Kästner, M. (1991) Reductive dechlorination of Tri- and tetrachloroethylenes depends on transition from aerobic to anaerobic conditions. Appl. Environ. Microbiol. 57: 2039-2036

Kim, Y., Arp, D.J. and Semprini, L. (2000) Chlorinated solvent cometabolism by butane-grown mixed culture. J. Environ. Eng. 126: 934-942

Koziollek, P., Bryniok, D. and Knackmuss, H. (1999) Ethene as an auxiliary substrate for the cooxidation of cis-1,2-dichloroethene and vinyl chloride. Arch. Microbiol. 172: 240-246

Krone, U.E., Laufer, K., Thauer, R.K. and Hogenkamp, H.P.C. (1989) Coenzyme F430 as a possible catalyst for the reductive dehalogenation of chlorinated C1 hydrocarbons in methanogenic bacteria. Biochemistry 28: 10061-10065

Lee, K.C. and Rittmann, B.E. (2002) Applying a novel autohydrogenotrophic hollow-fiber membrane biofilm reactor for denitrification of drinking water. Wat. Res. 36: 2040-2052

Lee, M.D., Odom, J.M. and Buchanan, R.J. (1998) New perspectives on microbial dehalogenation of chlorinated solvents: Insights from the field. Annu. Rev. Microbiol. 52: 423-452

Lendvay, J. M., Löffler, F.E., Dollhopf, M., Aiello, M.R., Daniels, G., Fathepure, B.Z., Gebhard, M., Heine, R., Helton, R. Shi, J., Krajmalnik-Brown, R., Major, Jr., C.L., Barcelona, M.J., Petrovskis, E., Hickey, R., Tiedje, J.M. and Adriaens, P. (2003) Bioreactive Barriers: A Comparison of Bioaugmentation and Biostimulation for Chlorinated Solvent Remediation. Environ. Sci. Technol. 37: 1422-1431

Lortie, L., Gould, W.D., Rajan, S., McCready, R.G..L. and Cheng, K.J. (1992) Reduction of selenate and selenite to elemental selenium by a *Pseudomonas stutzeri* isolate. Appl. Environ. Microbiol. 58: 4042-4044

Losi, M.E. and Frankenberger, W.T. (1997) Reduction of selenium oxyanions by *Enterobacter coalcae* strain SLD1a01: Reduction of selenate to selenite. Environ. Toxicol. Chem. 16: 1851-1857

Lovley, D.R. (1993) Dissimilatory metal reduction. Annu. Rev. Microbiol. 47: 263-293

Lovley, D.R. and Coates, J.D. (1997) Bioremediation of metal contamination. Current Opinion in Biotechnology 8: 285-289

Mackay, D.M. and Cherry, J.A. (1989) Groundwater contamination: pump-and-treat remediation. Environ. Sci. Technol. 28: 630-636

Macy, J.M., Lawson, S. and DeMoll-Decker, H. (1993) Bioremediation of selenium oxyanions in San Joaquin drainage water using *Thaura selenatis* in a biological reactor system. Appl. Microbiol. Biotechnol. 40: 588-594

Maiers, D.T., Wichlacz, P.L., Thompson, D.L. and Bruhn, D.F. (1988) Selenate reduction by bacteria from a selenium-rich environment. Appl. Environ. Microbiol. 54: 2591-2593

Major, D.W., Hodgins, E.W. and Butler, B.J. (1991) On-site Bioreclamation: Processes of Xenobiotic and Hydrocarbon Treatment; Hinchee, R.E., Olfenbuttel, R.F., Eds.: Butterworth-Heinemann: Boston.

Major, D.W., McMaster, M.L., Cox, E.E., Edwards, E.A., Dworatzek, S,M., Hendrickson, E.R., Starr, M.G., Payne, J.A. and Buonamici, L.W. (2002) Field Demonstration of Successful Bioaugmentation To Achieve Dechlorination of Tetrachloroethene To Ethene. Environ. Sci. Technol. 36: 5106-5116

Marsh, T.L. and McInerney, M.J. (2001) Relationship of hydrogen bioavailability to chromate and reduction in aquifer sediments. Appl. Environ. Microbiol. 67: 1517-1521

Muyzer, G.., Dewaal, E.C. and Uitterlinden, A.G. (1993) Profiling of complex microbial-populations by denaturing gradient gel-electrophoresis analysis of polymerase chain reaction-amplified genes-coding for 16s ribosomal-RNA. Appl. Environ. Microbiol. 59: 695-700

Maymo-Gatell, X., Nijenhuis, I. and Zinder, S.H. (2001) Reductive dechlorination of cis-1,2-dichloroethene and vinyl chloride by "Dehalococcoides ethenogenes". Environ. Sci. Technol. 35: 516-521

McCarty, P.L. and Wilson, J.T. (1992) Bioremediation of Hazardous Wastes; US EPA Office of Research and Development. EPA., Washington, D.C., pp 68; EPA/600/R-92/126

McNab, W.W. and Narasimhan, T.N. (1994) Degradation of chlorinated hydrocarbons and groundwater geochemistry - A field-study. Environ. Sci. Technol. 28: 769-775

Mikesell, M.D. and Boyd, S.A. (1990) Dechlorination of chloroform by Methanosarcina strains. Appl. Environ. Microbiol. 56: 1198-1201

Montzka, S.A., Spivakovsky, C.M., Butler, J.H., Elkins, J.W., Lock, L.T. and Mondeel DJ. (2000) New observational constraints for atmospheric hydroxyl on global and hemispheric scales. Science 288: 500-503

Narayan, B., Suidan, M.T., Gelderloos, A.B. and Brenner, R.C. (1993) Treatment of VOCs in high strength wastes using an anaerobic expanded-bed GAC reactor. Wat. Res. 27: 181-194

National Research Council (NRC) (2000) Natural Attenuation for Groundwater Remediation. National Academy Press, Washington, DC.

National Toxicology Program (1991) Sixth annual report on carcinogens. Research Triangle Park, NC: US Department of Health and Human Services

Nerenberg, R. (2003) Perchlorate removal from drinking water with a hydrogen-based, hollow-fiber membrane biofilm reactor. Ph.D. Dissertation at Northwestern University

Nerenberg, R., Rittmann, B.E. and Najm, I. (2002) Perchlorate reduction in a hydrogen-based membrane-biofilm reactor. J. Am. Water Works. Ass. 94: 103-114

Oldenhuis, R., Oedzes, J.Y., van der Waarde, J.J. and Janssen, D.B. (1991) Kinetics of chlorinated aliphatic hydrocarbons by Methylosinus trichosprium OB3b and toxicity of trichloethylene. Appl. Environ. Microbiol. 57: 7-14

Oldenhuis, R., Vink, R.L.J.M., Janssen, D.B. and Witholt, B. (1989) Degradation of chlorinated aliphatic hydrocarbons by Methylosinus trichosporium OB3b expressing soluble methane monooxygenase. Appl. Environ. Microbiol. 55: 2819-2826

Oliver, D.S., Brockman, F.J., Bowman, R.S. and Kieft, T.L. (2003) Microbial reduction of hexavalent chromium under vadose zone conditions. J. Environ. Qual. 32: 317-324

Oremland, R.S., Steinberg, N.A., Maest, A.S., Miler, L.G.. and Hollibaugh, J.T. (1990) Measurement of in situ rates of selenate removal by dissimilatory bacterial reduction in sediments. Environ. Sci. Technol. 24: 1157-1164

Palmer, C.D. and Wittbrodt, P.R. (1991) Processes affecting the remediation of chromium-contaminant sites. Environmental Health Perspectives. 92: 25-40

Parsons, F., Lage, G.B. and Rice, R. (1985) Biotransformation of chlorinated organic solvents in static microcosms. Environ. Toxicol. Chem. 4: 739-742

Postgate, J. (1984) The sulphate-reducing bacteria, pp. 56-100. Cambridge: Cambridge University Press

Rege, M.A., Yonge, D.R., Mendoza, D.P., Peterson, J.N., Bereded-Samuel, Y., Johnstone, D.L., Apel, W.A. and Barnes, D.P. (1999) Selenium reduction by a denitrifying consortium. Biotech. Bioeng. 62:479-484

Rittmann, B.E. and McCarty, P.L. (2001) Environmental Biotechnology – Principles and applications. New York, McGraw-Hill

Semprini, L., Kampbell, D.H. and Wilson, J.T. (1995) Anaerobic transformation of chlorinated aliphatic-hydrocarbons in a sand aquifer based on spatial chemical-distributions. Water Resources Research. 31: 1051-1062

Sherwood Lollar, B., Slater, G.F., Sleep, B., Witt. M., Klecka, G.M., Harkness, M. and Spivack, J. (2001) Stable Carbon Isotope Evidence for Intrinsic Bioremediation of

Tetrachloroethene and Trichloroethene at Area 6, Dover Air Force Base. Environ. Sci. Technol. 35: 261-269

Smith, L.H. and McCarty, P.L. (1997) Laboratory evaluation of a two-stage treatment system for TCE cometabolism by a methane-oxidizing mixed culture. Biotech. Bioeng. 55: 650-659

Smith, W.L. and Gadd, G.M. (2000) Reduction and precipitation of chromate by mixed culture sulphate-reducing bacterial biofilms. J. Appl. Microbiol. 88:983-991

Speitel, G.E. and Leonard, J.M. (1992) A sequencing biofilm reactor for the treatment of chlorinated solvents using methanotrophs. Water Environ. Res. 64: 712-719

Stickley, D.P. (1970) The effect of chloroform in sewage on the production of gas from laboratory digestors. Wat. Pollut. Contr. 69: 585-590

Tsai, Y.L. and Rochelle, P.A. (2001) Extraction of nucleic acids from environmental samples. In: *Environmental Molecular Microbiology: Protocols and Application*. P.A. Rochelle (ed) Horizon Scientific Press, Norfolk, England, 15-30

USEPA (1992) Integrated risk information system (IRIS), Cincinnati, OH: Environmental Criteria and Assessment Office

USEPA (1995) National Primary Drinking Water Regulations: Technical Fact sheet on: Trichloroethylene, USPEA Web: http://www.epa.gov/OGWDW/dwh/t-voc/trichlor.html

USEPA, Office of Pollution Prevention and Toxics (TS-799) (1991) 1991 Toxics Release Inventory – Public Data Release, Washington, DC.

Vainshtein, M., Kuschk, P., Mattusch, J., Vatsourina, A. and Wiessner, A. (2003) Model experiments on the microbial removal of chromium from contaminated groundwater. Wat. Res. 37: 1401-1405

Vannelli, T., Logan, M., Arciero, D.M. and Hooper, A.B. (1990) Degradation of halogenated aliphatic compounds by the ammonia-oxidizing bacterium *Nitrosomonas europaea*. Appl. Environ. Microbiol. 56: 1169-1171

Verce, M.F., Ulrich, R.L. and Freedman, D.L. (2000) Characterization of an isolate that uses vinyl chloride as a growth substrate under aerobic conditions. Environ. Sci. Technol. 66: 3535-3542

Vogel, T.M. and McCarty, P.L. (1987) Abiotic and biotic transformations of 1,1,1-trichloroethane under methanogenic conditions. Environ. Sci. Technol. 21: 1208-1213

Vogel, T.M., Criddle, C.S. and McCarty, P.L. (1987) Transformations of halogenated aliphatic compounds. Environ. Sci. Technol. 21: 722-736

Wan, H.S., Hao, O.J. and Kim, H. (2001) Environmental factors affecting selenite reduction by a mixed culture. J. Environ. Eng. 127: 175-178

Wang, P.C., Mori, T., Komori, K., Sasatsu, M., Toda, K. and Ohtake, H. (1989) Isolation and characterization of an Enterobacter cloacae strain that reduces hexavalent chromium under anaerobic conditions. Appl. Microbiol. Biotechnol. 55: 1665-1669

Westrick, J.J., Mello, J.W. and Thomas, R.F. (1984) The groundwater supply survey. J. Am. Water Works. Ass. 76: 52-29

Wilson, J.T. and Wilson, B.H. (1985) Biotransformation of trichloroethylene in soil. Appl. Environ. Microbiol. 49: 242-235

Wrenn, B. A. and B. E. Rittmann (1995). A model for the effects of primary substrates on the kinetics of reductive dehalogenation. Biodegradation 6: 295-305.

Wrenn, B. A. and B. E. Rittmann (1996). Evaluation of a mathematical model for the effects of primary substrates on reductive dehalogenation kinetics. Biodegradation 7: 49-64.

Yang, J. and Speece, .R.E. (1986) The effect of chloroform toxicity on methane fermentation. Wat. Res. 20: 1273-1279

APPENDIX A

State of California—Health and Human Services Agency

Department of Health Services

DIANA M. BONTÁ, R.N., Dr. P.H.
Director

GRAY DAVIS
Governor

June 16, 2003

Samer Adham, Ph.D.
MWH Global
555 East Walnut Street
Pasadena, CA 91101

Dear Dr. Adham: Samer

MEMBRANE BIOREACTORS FOR PERCHLORATE REMOVAL

Thank you for submitting your letter of March 17, 2003 (with the subject line: "Review of an Innovative Perchlorate Treatment Technology") detailing your work with membrane bioreactors and perchlorate reduction. As you are aware, the Department has accepted the use of biological treatment (fluidized bed reactors) for the reduction of perchlorate concentrations in sources used for the production of potable water supply. However, the Department has placed several stipulations on the use of biological treatment that might apply to your proposed membrane technology. The Department's Water Treatment Committee has reviewed your letter and has the following comments for your consideration.

1. Water production from the biological treatment process should minimize changes in production flow rates (e.g., a plant operated 24 hours a day, 7 days a week, 365 days a year to provide a minimum production of water (base loading or base flow)).

2. If variability in flow and composition for extended periods of time cannot be controlled and minimized, then product water should be stored to allow analysis before releasing the water to the distribution system.

3. Site-specific tests are required to determine the impact of seasonal and temporal variations in water quality (temperature, available micro and macro nutrients, etc.) on process performance. For example, it is anticipated the hydrogen requirement varies as a function of source water quality, so the impact(s) of variable nitrate concentrations (in time and magnitude) on finished water quality needs to be evaluated.

Drinking Water Technical Programs Branch, 2151 Berkeley Way, Room 458, Berkeley, CA 94704-1011
(510) 540-2158 FAX (510) 540-2152
DHS Internet Address: www.dhs.ca.gov Program Internet Address: www.dhs.ca.gov/ps/ddwem

4. Since the microorganisms are endemic to the groundwater, it is not necessary to identify and characterize the microbial population.

5. All chemicals used in the system must be NSF standard 60 certified by an ANSI accredited laboratory, including the hydrogen gas.

6. It is recommended that all components used in the manufacture of the reactor vessel that come into direct contact with the source water be NSF standard 61 certified by an ANSI accredited laboratory.

7. It is also recommended that development continue on a reliable hydrogen contro system that would allow feed-forward control of the hydrogen based on measured changes in composition and flow.

8. Treatment following biological perchlorate removal, at a minimum, may need to meet the disinfection requirements of the Surface Water Treatment Rule (Title 22 of the California Code of Regulations, Div. 4, Chapter 17) due to the possibility that opportunistic bacterial pathogens might survive and/or reproduce within the reactor vessel.

9. On-line monitoring systems for perchlorate and nitrate should be incorporated into process design for improving process control.

10. If VOCs, SOCs, or other organic compounds are present, it may be necessary to provide additional organics removal (e.g., advanced oxidation (UV/H_2O_2) and/or granular activated carbon) downstream of the MBR as an independent unit treatment process.

11. Designation as a best available treatment technology will require, by statute under the Health and Safety Code (Part 12 Chapter 4 Article 3 Section 116370), at a minimum, a full-scale application of the technology.

12. Your study is setup to demonstrate long-term steady-state operation, but what happens if there are short-term interruptions in the hydrogen feed or the perchlorate concentration? How will the treatment process be started after a power outage of a few hours? Non steady-state operation will be a critical issue. After the membranes are cleaned, how long will it take for the process to recover and start producing low perchlorate concentration product? This means looking at production stoppages and determining their impact (magnitude and duration) on product water quality (time dependent).

13. There are practical issues beyond the demonstration of the technology for perchlorate reduction. The residence time is stated as 7-30 minutes. How large must the system be (how many modules) to get any sort of production out of it?

14. Based on the kinetics, what would you say the minimum substrate concentration (perchlorate) would be, i.e., based on the biochemical reaction kinetics how much perchlorate would be left in the water?

15. The production of hydrogen sulfide is dismissed by stating that aeration and/or disinfection will readily oxidize it to sulfate. Theoretically, that is what happens. However, in actual practice, unless there is a large excess of oxidant, the oxidation is incomplete, producing intermediate thio compounds (e.g., tetrathionates) some of which cause objectionable taste and odor.

16. The comment is made that the process reduces perchlorate to chloride. Has this been demonstrated to be a 100% efficient reaction? If so, what was the evidence that provided the assurance that this reaction is going to completion?

17. What controls the maximum loading rate on the MBR, i.e., what limits or controls the efficacy of the MBR? How do perchlorate or other compounds impact the loading rate on the MBRs?

There may also be regulatory issues outside our Department's jurisdiction, such as worker health and safety with respect to the use and storage of hydrogen gas on-site.

The membrane bioreactor does appear to be a promising technology for perchlorate reduction. The Department looks forward to future communications from you regarding this technology. We hope these comments provide you with the feedback you are seeking and help direct future research so that the regulatory and permitting issues raised, can be addressed. Should you have any questions regarding the content of this letter, please free to contact me at (510) 849-5050.

Very truly yours,

Richard H. Sakaji, PhD, PE
Senior Sanitary Engineer

cc: WT Committee
chron

PERCHLORATE WORKGROUP CONFERENCE CALL – AWWARF/NWRI MBFR

MWH

NORTHWESTERN UNIVERSITY

CALIFORNIA DEPARTMENT OF HEALTH SERVICES WATER TREATMENT COMMITTEE

Workshop Minutes

SEPTEMBER 23, 2003

10:00 AM – 12:00 PM

Present:
Samer Adham – MWH
Geno Lehman – MWH
Kuang-Ping Chiu – MWH
Bruce Rittmann – Northwestern University
Rick Sakaji - CaDHS
Brian Bemados - CaDHS
Carl Carlucci - CaDHS
Cindy Forbes - CaDHS
Carl Lischeske - CaDHS
Jeffry Stone - CaDHS
Kurt Souza - CaDHS
Richard Haberman - CaDHS
Shu-Fang Orr - CaDHS
Sharon Wong - CaDHS

Presentation and Discussion:

Introduction and Project Background (Samer Adham/Rick Sakaji)

- Introduction of CaDHS committee
- Background of MBfR project and teaming from AwwaRF to NWRI

Membrane Biofilm Reactor Process Overview (Samer Adham/Geno Lehman)

- MBfR uses special hollow fiber membranes to deliver hydrogen gas supplied to the lumens of the fibers to the biofilm growing on the outside of the fibers.
- The MBfR is an anaerobic process and is followed by aeration and filtration (media or membrane)
- Bubbling of hydrogen is eliminated because the gas diffuse through the membrane directly into the biofilm
- Laboratory prototype experiments were performed at Northwestern University using a bench-scale MBfR.
- The well studies perchlorate reduction pathway reduces ClO4 -> ClO3 -> ClO2 -> Cl + O2.
- Initial response to perchlorate in a denitrifying MBfR was favorable as perchlorate was able to be reduced from 1500 µg/L to below 10 µg/L.

- Following bench-scale confirmation of perchlorate reduction using the MBfR, a pilot-scale system was built by MWH and operated at La Puente in southern California.
- Using a two reactor in series design for research purposes at pilot-scale, influent perchlorate (60 μg/L) was reduced to below the 4 μg/L CaDHS action limit.
- In addition, a high degree of correlation was observed for the actual and theoretical hydrogen consumption rates indicating nearly 100 percent hydrogen usage efficiency.
- Recent efforts have focused on determining the applicability of the MBfR to additional oxidized contaminants. Preliminary screening experiments have been favorable.

Notes:

~ Question about membrane process (Stone). Clarified the point that water flows around the membrane and not through, as in typical filtration processes.
~ General (Slide 14). The influent and effluent colors on the figure are switched. As is, the graph indicates that perchlorate is being produced. Correction: 1500 μg/L is reduced to below 10 μg/L.
~ General (Slide 15). The pilot trailer was temperature controlled to maintain an ambient temperature of 21 °C. Seasonal temperature changes during operation did not affect operation.
~ General (Slide 18). Question (Lischeske) as to how radionuclides can be removed by the MBfR. During the reduction process, radionuclides for precipitates which can be further removed from the MBfR by a solids removal system.

Response to CaDHS Review (Samer Adham/Bruce Rittmann)

- Comments were provided to the MBfR Project team in a memo from CaDHS data June 16, 2003.
- Individual comments were addressed. See presentation.

Notes:

~ Rittmann (Comment 7 – H2 control). Hydrogen control is a self-regulating process which is the advantage of the MBfR. In addition, since H_2 cannot be overdosed due to its low solubility in water, the issues associated with overdosing of similar organic donors (i.e., acetate, methanol, etc.) are not an issue.
~ Fang (Comment 9 – online ClO_4 monitoring). Castaic Lake currently uses a Dionex DX800 configured for on-line ClO_4. In addition, sophisticated column switching systems can be utilized to analyze ClO_4 and NO_3.
~ Sakaji (Comment 9 0 online ClO_4 monitoring). Online ClO_4 monitoring will be required for full-scale installation of the treatment system. The currently DHS approved FBR system required the addition of online ClO_4 analysis.
~ General (Comment 12 – process interruptions). Process shutdowns from a few hours to up to 1 week have been observed at pilot scale. The MBfR has been found to be an extremely robust process, which can quickly recover. Short-term interruptions (<24 hours) have been demonstrated to recover within a few HRTs (up to 30 min/HRT). Longer interruptions (i.e., 1-week shutdown, aggressive acid clean) required 24-48 hours to fully recover.

Action Items:

~ CaDHS will provide MWH/Northwestern Team with contact with Dionex and Castaic Lake for online ClO_4 analysis
~ MWH will continue to address comments, which will be evaluated under current research efforts.

Review of NWRI Research Project (Samer Adham/Bruce Rittmann)

- Project Objective: to evaluate and optimize the MBfR process for the removal of additional inorganic and organic oxidized contaminants
- Discussed the main project tasks: 1) bench-scale screening, 2) hydraulic modeling, and 3) regulatory review

Notes:

~ Bench-scale testing and hydraulic modeling is currently underway

~ This conference call is the first step towards accomplishing Task 3. A follow up call between the Project team and CaDHS will occur at the end of the NWRI research efforts (~ 1 year from now)

Discussion and Closing

Comment

~ Sakaji. CaDHS is comfortable with the responses to comment in the letter (date June 16, 2003). CaDHS requests that the comments and responses be documented by incorporating them into the NWRI project final document.

~ Sakaji. To date, the status of the MBfR research has been bench- and pilot-scale testing. The next step for developing conditional acceptance of this technology is to demonstrate the MBfR process at full-scale.

Question

~ Bernados. Is filtration really necessary? There is a difference between addition of filtration for purposes of removing sloughed biomass and treating the water for the SWTR.

Response

~ MWH/NU. The addition of a filtration step has been a conservative approach specifically for the treatment of groundwater for potable use. The project team will investigate this further in current efforts and evaluate the addition of a filtration process for both the capture of sloughed biomass and meeting SWTR requirements. In addition, extensive post-MBfR process simulate distribution tests will be performed to further address the SWTR.

Question

~ Adham. According to CaDHS, what is the potential for the MBfR to be approved for a 0.5 – 1.0 MGD system?

Response

~ Haberman. Given the current state of the technology presented, there is a high possibility for approval of the MBfR for groundwater. The best application (today) would be for the treatment of nitrate-contaminated groundwaters in CA. To be approved, the process would need filtration and disinfection.

General:

~ Several members of CaDHS agree with Haberman that treatment of nitrate is a more immediate application as opposed to perchlorate

~ (Lischeske) Several site in central CA are contaminated with NO_3 and the MBfR could be applied.

~ Several site in California are contaminated with PPCP and NO_3 in which the MBfR could be a potential treatment option

~ Another recommended future application would be a groundwater recharge project for recycled water containing high NO_3 and DOC.

~Sakaji. As stated in the previous letter containing process comments, the MBfR is a promising technology. Regarding future approval of the MBfR, CaDHS is now more comfortable with biological treatment processes following the acceptance of the fluidized bed reactor (FBR) for the reduction of perchlorate concentration in sources used for the production of potable water supply. Approval of the MBfR should easily follow the FBR's precedent and may just be a simple twist in the regulatory review process to get approved.